

**Structure of charmed baryons studied by pionic decays**Hideko Nagahiro,<sup>1,2</sup> Shigehiro Yasui,<sup>3</sup> Atsushi Hosaka,<sup>2,4</sup> Makoto Oka,<sup>3,5</sup> and Hiroyuki Noumi<sup>2</sup><sup>1</sup>*Department of Physics, Nara Women's University, Nara 630-8506, Japan*<sup>2</sup>*Research Center for Nuclear Physics (RCNP), Osaka University, Ibaraki, Osaka 567-0047, Japan*<sup>3</sup>*Department of Physics, Tokyo Institute of Technology, Meguro 152-8551, Japan*<sup>4</sup>*J-PARC Branch, KEK Theory Center, KEK, Tokai, Ibaraki 319-1106, Japan*<sup>5</sup>*Advanced Science Research Center, Japan Atomic Energy Agency, Tokai, Ibaraki 319-1195, Japan*

(Received 6 September 2016; published 23 January 2017)

We investigate the decays of the charmed baryons aiming at the systematic understanding of hadron internal structures based on the quark model by paying attention to heavy quark symmetry. We evaluate the decay widths from the one-pion emission for the known excited states,  $\Lambda_c^*(2595)$ ,  $\Lambda_c^*(2625)$ ,  $\Lambda_c^*(2765)$ ,  $\Lambda_c^*(2880)$ , and  $\Lambda_c^*(2940)$ , as well as for the ground states  $\Sigma_c(2455)$  and  $\Sigma_c^*(2520)$ . The decay properties of the lower excited charmed baryons are well explained, and several important predictions for higher excited baryons are given. We find that the axial-vector-type coupling of the pion to the light quarks is essential, which is expected from chiral symmetry, to reproduce the decay widths especially of the low-lying  $\Lambda_c^*$  baryons. We emphasize the importance of the branching ratios of  $\Gamma(\Sigma_c^*\pi)/\Gamma(\Sigma_c\pi)$  for the study of the nature of higher excited  $\Lambda_c^*$  baryons.

DOI: [10.1103/PhysRevD.95.014023](https://doi.org/10.1103/PhysRevD.95.014023)**I. INTRODUCTION**

Understanding of the internal structure of hadrons is an important subject in hadron physics. One of the most important problems is to identify the effective degrees of freedom which should play essential roles at low energies, because the bare quarks do not appear at such a scale due to the color confinement of QCD. To identify the effective degrees of freedom should serve not only for the understanding of the QCD vacuum properties, but also be useful to explain and predict experimental data with simple physical terms. In this respect, what we are aiming at is to establish the economized effective degrees of freedom for various phenomena of the strong interaction physics [1,2].

The charmed baryons, containing a single heavy charm quark, is a good place to study the hadron structure. One of the important features is the spin symmetry of the heavy quark. QCD predicts that the spin-dependent interaction of the heavy quark is suppressed by  $1/m_Q$  and thus in the infinite  $m_Q$  limit, the heavy quark spin is decoupled from the dynamics of the light quarks. The dynamical decoupling of the light quark spin and the heavy quark spin is the heavy quark symmetry (HQS) [3].

In the heavy quark limit, the total spin  $j$  of the light degrees of freedom (so-called brown muck in the literature) is conserved [3,4]. It contains not only the spins of the light (anti)quarks and their angular momenta but also gluon spins. Combining the spin  $j$  of the light degrees of freedom and the spin of a heavy quark, heavy hadrons are classified into a single state with the total spin  $J = 1/2$  for  $j = 0$  and two degenerate states with the total spin  $J = j \pm 1/2$  for  $j \geq 1/2$ . The former is called the HQS singlet, and the latter

is called the HQS doublet. The classification based on the HQS is useful for the investigation of the heavy hadrons, because the spin of the light degrees of freedom serves as an additional conserved quantum number reflecting the internal structure of the heavy hadrons. The HQS appears in many properties of heavy hadrons, such as the mass spectrum and the decay branching ratios.<sup>1</sup>

There is another interesting feature of the charmed baryons. In the quark model description, we have two different orbital motions in the low-energy excitations. One is the relative motion between two light quarks, the so-called  $\rho$ -mode. The other is the one between the center of mass of the two light quarks and the charm quark, the so-called  $\lambda$ -mode. Owing to the mass difference of the light and heavy quarks, the excitation energies of the  $\lambda$ - and  $\rho$ -modes are kinematically well separated, and the internal excitations are dominated exclusively by either the  $\rho$ -mode or the  $\lambda$ -mode with only small mixing [23]. This contrasts with light quark baryons where the two modes generally mix largely, and thus is the reason that we can study the two basic modes exclusively in the heavy baryons.

In general, internal structures of hadrons are reflected not only in mass spectrum but also in various transition properties such as productions and decays. Among them, two-body decay processes through the one-pion emission are particularly interesting due to the following reasons. (i) The pion couples only to the light quarks, and the charm quark behaves simply as a spectator. The dynamics of the

<sup>1</sup>The heavy quark symmetry can be applied also to exotic heavy hadrons such as hadronic molecules [5–15] as well as to the heavy hadrons in the nuclear medium [15–21]. See Ref. [22] as a review for the latter.

pion is governed by chiral symmetry in a unique manner. Therefore, the transitions accompanying pion emission should bring important information about the dynamics of the two light quarks in a heavy baryon. This is also helpful to understand diquark properties in a heavy baryon. (ii) Some low-lying states of excited charmed baryons have significantly smaller excitation energies than light baryon excitations, and the emitted pion carries only a small momentum. Therefore, the pion emission from the excited charmed baryons is a good place to study the quark-pion interaction, which should be well determined by the low-energy chiral dynamics. This can be checked by comparing the theoretical results with the observed decays of the low-lying charmed baryons.

In this paper we consider the pion emission decays from the orbitally excited charmed baryons<sup>2</sup>  $\Lambda_c^*(2595)$ ,  $\Lambda_c^*(2625)$ ,  $\Lambda_c^*(2765)$ ,  $\Lambda_c^*(2880)$ ,  $\Lambda_c^*(2940)$  into  $\Sigma_c(2455)\pi$  and  $\Sigma_c^*(2520)\pi$ , and those from orbital ground state charmed baryons  $\Sigma_c(2455)$  and  $\Sigma_c^*(2520)$  into  $\Lambda_c(2286)\pi$ . The decay paths are summarized in Fig. 1. To estimate the decay widths numerically, we employ a nonrelativistic constituent quark model with a harmonic oscillator potential as the quark confinement force. The model is rather simple but we expect that essential and universal features can be extracted.

There are previous works investigating strong decays of charmed baryons [3,18,25–31]. In Ref. [30], based on heavy hadron chiral perturbation theory the importance of heavy quark symmetry is discussed in the heavy quark limit. In Ref. [18], including the correction terms from the next-to-leading order  $\mathcal{O}(1/m_Q)$ , relationships between decay widths in several decay channels were obtained. In Ref. [31], nonrelativistic quark model calculations were performed and decays of various quark model states were investigated. In the present study, we will also employ the nonrelativistic quark model. It is worthwhile to emphasize the difference between the works in Ref. [31] and ours. In Ref. [31], the baryon wave functions are constructed in the so-called  $LS$  coupling scheme, while we do so in the  $jj$  coupling scheme where the total spin  $j$  of the light degrees of freedom is first formed. In doing so, we will derive various relations and selection rules in relation to HQS.

In a similar fashion, the one-pion emission of the heavy baryons has been investigated in Ref. [32] (see also [33]). There the constituent quark model was referred to in order to derive various relations among couplings between the heavy baryons and pion with respect to HQS also. Then effective coupling strengths appeared there were evaluated by comparing their amplitudes with available experimental data. In our approach here, the one-pion emission decay widths are explicitly evaluated by using quark model wave functions of the harmonic oscillator type with a few model

<sup>2</sup>In this article, we express the ground and excited charmed baryons as  $Y_c$  and  $Y_c^*$ .

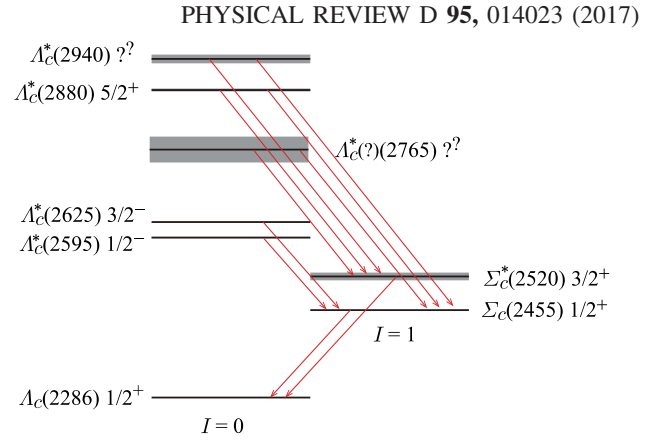


FIG. 1. Level structure of the charmed baryons with isospin  $I = 0$  and  $I = 1$   $Y_c(mass)J^P$  considered in this study. The hatched squares denote their total decay widths in Particle Data Group (PDG) [24]. The arrows indicate the possible decay paths with one-pion emission evaluated in this study.

parameters. Our quark model calculations also satisfy the heavy quark symmetry.

In our study, we will shed light upon the following issues. First, we check the validity of the present framework by calculating the decay widths of the two  $\Sigma_c$  baryons,  $\Sigma_c(2455)(J^P = 1/2^+)$  and  $\Sigma_c^*(2520)(J^P = 3/2^+)$ , which are the orbital ground state of charmed baryons. These baryons decay into  $\Lambda_c(2286)\pi$  as the only possible channel in strong decay. Because both the initial and final charmed baryon states are in the orbital ground states in the quark model, those charmed baryons are good objects for confirmation of the validity of our formalism for the one-pion emission. We will see that our results are in reasonably good agreement with the experimental values.

Second, we investigate the decay properties of  $\Lambda_c^*(2595)(J^P = 1/2^-)$  and  $\Lambda_c^*(2625)(J^P = 3/2^-)$  as the lowest-lying orbital excitations in a  $p$ -wave. They are interesting because they have the subcomponent, the spin-0 diquark system, which is moving in the  $p$ -wave orbital of the  $\lambda$ -mode [27,34,35]. They have been observed in  $e^+e^-$  collisions and  $p\bar{p}$  collisions [36–38] as well as in photo-productions [39]. An interesting feature of them is that the  $\Lambda_c^*(2595)(1/2^-)$  baryon has a considerably large decay width into the  $\Sigma_c\pi$  channel although its phase space is very small. In contrast,  $\Lambda_c^*(2625)(3/2^-)$  has a very small width although there is sufficiently large phase space in its decay channel  $\Sigma_c\pi$ . We show that the quark model description with the  $\lambda$ -mode can explain these decay properties very well for these low-lying  $Y_c$  states. We find that, to achieve good agreement, the  $\pi qq$  interaction Lagrangian of the derivative coupling (axial-vector coupling) is needed to reproduce the experimental decay width. This strongly implies that the nonlinear chiral dynamics works for the pion and constituent quarks. We will present that decay properties of  $\Lambda_c^*(2595)$  in particular are much affected by the isospin breaking effect near the thresholds.

Third, we study higher excited charmed baryons,  $\Lambda_c^*(2765)$ ,  $\Lambda_c^*(2880)$ , and  $\Lambda_c^*(2940)$ . Because their spins and parities are not fully determined experimentally, we consider various patterns of assignments of  $1/2^\pm$ ,  $3/2^\pm$ , and  $5/2^\pm$  which are formed by the quark model. By comparing the resulting decay widths with existing experimental data, we will see that several assignments of spin and parity will be excluded.

Finally, we will pay special attention to  $\Lambda_c^*(2880)$  for the determination of its spin and parity. In PDG [24], the spin of the  $\Lambda_c^*(2880)$  is  $5/2$ , which is determined by the angular distribution of the  $\Sigma_c(2455)\pi$  decay [24,40], and the positive parity is inferred from the agreement of the observed decay branching ratio  $\Sigma_c^*(2520)/\Sigma_c(2455)$  in comparison to the prediction from heavy quark symmetry [3,30,40]. As carefully argued in Ref. [30], however, the possible  $p$ -wave contribution was simply ignored in the evaluation of the branching ratio. We show that the many configurations for the  $\Lambda_c^*$  baryons with  $J^P = 5/2^+$  are turned out to be incompatible with the present experimental data [40] if the  $p$ -wave contribution is properly considered. We find that only one configuration leads to a result consistent with the data where  $p$ -wave contribution vanishes due to the selection rule working for the pion emission between diquarks, the occurrence of which is a unique feature of heavy baryons where a heavy quark behaves as a spectator, namely in heavy quark symmetry.

This article is organized as follows. In Sec. II, we explain wave functions of the charmed baryons employed in our constituent quark model. In Sec. III we present the formalism for the one-pion emission decay of the charmed baryon. We show our numerical results for the decay widths in Sec. IV. Finally, Sec. V is devoted to a summary.

## II. BARYON WAVE FUNCTIONS WITHIN THE QUARK MODEL

We construct the baryon wave functions in a scheme inspired by the heavy quark symmetry. Namely, first we construct a wave function using light degrees of freedom, which is then combined with the heavy quark to form the total baryon wave functions. In this manner, we will be able to see in a transparent manner various relations and selection rules which are valid in the heavy quark limit. Let us start with the harmonic oscillator Hamiltonian for the orbital wave function,

$$H = -\sum_{i=1}^3 \frac{\vec{\nabla}_i^2}{2m_i} + \sum_{i \neq j} \frac{k}{2} (\vec{r}_i - \vec{r}_j)^2, \quad (1)$$

where  $\vec{r}_i$  are the spatial coordinates of the  $i$ th quark of mass  $m_i$  and  $k$  the spring constant.

Quark 1 and quark 2 denote the two light quarks of mass  $m$  ( $m_1 = m_2 = m$ ), and quark 3 the charm quark of mass  $M$  ( $m_3 = M$ ). The Hamiltonian can be divided into one for the

center-of-mass motion  $\vec{X}$  and those for the relative motions  $\vec{\rho}$  and  $\vec{\lambda}$  as

$$H = H_G + H_\rho + H_\lambda, \quad (2)$$

where

$$H_G = -\frac{\vec{\nabla}_X^2}{2(2m + M)}, \quad (3a)$$

$$H_\rho = -\frac{\vec{\nabla}_\rho^2}{2m_\rho} + \frac{m_\rho \omega_\rho^2}{2} \vec{\rho}^2, \quad (3b)$$

$$H_\lambda = -\frac{\vec{\nabla}_\lambda^2}{2m_\lambda} + \frac{m_\lambda \omega_\lambda^2}{2} \vec{\lambda}^2. \quad (3c)$$

Here, the coordinate of the center of mass  $\vec{X}$  is defined as

$$\vec{X} = \frac{1}{2m + M} (m(\vec{r}_1 + \vec{r}_2) + M\vec{r}_3), \quad (4)$$

and  $\vec{\rho}$  and  $\vec{\lambda}$  are the Jacobi coordinates defined as

$$\vec{\rho} = \vec{r}_1 - \vec{r}_2, \quad (5a)$$

$$\vec{\lambda} = \frac{1}{2}(\vec{r}_1 + \vec{r}_2) - \vec{r}_3. \quad (5b)$$

As indicated in Fig. 2,  $\vec{\rho}$  is the relative coordinate between the two light quarks (quark 1 and quark 2), and  $\vec{\lambda}$  is the relative coordinate between the center of mass of the two light quarks and the charm quark.

The reduced masses  $m_\lambda$  and  $m_\rho$  are defined by

$$m_\rho = \frac{m}{2}, \quad m_\lambda = \frac{2mM}{2m + M}, \quad (6)$$

and the frequencies of the oscillator for the  $\lambda$ - and  $\rho$ -modes by

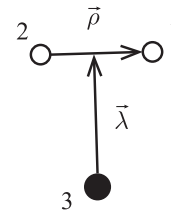


FIG. 2. Definitions of the Jacobi coordinates  $\vec{\rho}$  and  $\vec{\lambda}$ . The quarks 1 and 2 are the light quarks, and 3 the heavy (charm) quark.

$$\omega_\rho = \sqrt{\frac{3k}{m}}, \quad \omega_\lambda = \sqrt{\frac{k(2m+M)}{mM}}. \quad (7)$$

Orbital wave functions of the three-quark state are expressed by a simple product of the eigenfunctions of the separated Hamiltonians

$$\Psi(\vec{r}_1, \vec{r}_2, \vec{r}_3) = \psi_\lambda(\vec{\lambda})\psi_\rho(\vec{\rho})e^{i\vec{P}\cdot\vec{X}}, \quad (8)$$

where  $\vec{P}$  is the total momentum of the three-quark state, and  $\psi_\lambda(\vec{\lambda})$  and  $\psi_\rho(\vec{\rho})$  the wave functions of the Jacobi coordinates  $\vec{\lambda}$  and  $\vec{\rho}$ . The wave functions of the harmonic oscillator are given by

$$\psi_{n\ell m}(\vec{x}) = R_{n\ell}(r)Y_{\ell m}(\hat{x}), \quad (9)$$

where the radial function  $R_{n\ell}(r)$  is summarized in Appendix A and  $Y_{\ell m}$  is the spherical harmonics. We will call the excitation with either  $n_\lambda \neq 0$  (radial excitation) or  $\ell_\lambda \neq 0$  (orbital excitation) the  $\lambda$ -mode. This is also the case for the  $\rho$ -mode. When both the  $\lambda$ -mode and the  $\rho$ -mode happen, this is called the  $\lambda\rho$ -mode.

The full wave functions of baryons are constructed by products of the isospin (flavor) part, the spin part, and the orbital part. For the isospin part, we introduce the notation  $D^I_{(I_z)}$  for the two light quarks as

$$D^0: \left\{ D^0_0 = \frac{1}{\sqrt{2}}(ud - du) \right\}, \quad (10)$$

for an  $I = 0$  state, and

$$D^1: \left\{ D^1_1 = uu, D^1_0 = \frac{1}{\sqrt{2}}(ud + du), D^1_{-1} = dd \right\}, \quad (11)$$

for  $I = 1$  states. The flavor wave function of the  $\Lambda_c$  baryons having  $I = 0$  is then expressed by  $D^0c$  ( $c$  stands for the charm quark), and that of the  $\Sigma_c$  baryons with  $I = 1$  by  $D^1c$ .

Similarly, the spin wave functions of the two light quarks are expressed by  $d^s_{(s_z)}$ ,

$$d^0: \left\{ d^0_0 = \frac{1}{\sqrt{2}}(\uparrow\downarrow - \downarrow\uparrow) \right\}, \quad (12)$$

$$d^1: \left\{ d^1_1 = \uparrow\uparrow, d^1_0 = \frac{1}{\sqrt{2}}(\uparrow\downarrow + \downarrow\uparrow), d^1_{-1} = \downarrow\downarrow \right\}. \quad (13)$$

For the charm quark spin, we use the symbol  $\chi_c$  for either spin-up or -down.

By making use of these expressions, the full wave functions of the  $\Lambda_c(J)$  and  $\Sigma_c(J)$  with total spin  $J$  are constructed as

$$\Lambda_c(JM) = [[\psi_{n_\lambda\ell_\lambda m_\lambda}(\vec{\lambda})\psi_{n_\rho\ell_\rho m_\rho}(\vec{\rho}), d]^j, \chi_c]_M^J D^0c, \quad (14)$$

$$\Sigma_c(JM) = [[\psi_{n_\lambda\ell_\lambda m_\lambda}(\vec{\lambda})\psi_{n_\rho\ell_\rho m_\rho}(\vec{\rho}), d]^j, \chi_c]_M^J D^1c \quad (15)$$

by antisymmetrizing the light quark part including the color part, which is not explicitly shown here. The total spin  $J$  of the charmed baryon is given by the sum of the spin of the charm quark and the ‘‘total’’ angular momentum  $j$  of the remaining part (hereafter referred to as ‘‘light-component spin  $j$ ’’ or simply ‘‘light spin  $j$ ’’), which is obtained by composing the orbital angular momenta  $\ell_\lambda$  and  $\ell_\rho$  and diquark spin  $d$ . For example, the wave functions of the orbital ground state for the charmed baryons are given by

$$\Lambda_c(1/2^+) = [[\psi_{0s}(\vec{\lambda})\psi_{0s}(\vec{\rho}), d^0]^0, \chi_c]^{1/2} D^0c, \quad (16)$$

$$\Sigma_c(1/2^+) = [[\psi_{0s}(\vec{\lambda})\psi_{0s}(\vec{\rho}), d^1]^1, \chi_c]^{1/2} D^1c, \quad (17)$$

and

$$\Sigma_c^*(3/2^+) = [[\psi_{0s}(\vec{\lambda})\psi_{0s}(\vec{\rho}), d^1]^1, \chi_c]^{3/2} D^1c. \quad (18)$$

In Table I, we summarize the quark configurations for the charmed baryons considered in this article. The observed  $\Lambda_c$  excited states  $\Lambda_c^*(2595)$  and  $\Lambda_c^*(2625)$  baryons are, due to their small excitation energies, assigned to be the  $p$ -wave excitations of the  $\lambda$ -mode ( $n_\lambda = 0$ ,  $\ell_\lambda = 1$ ) with a spin-0 diquark ( $d^0$ ). Their quark configurations are given by

$$\Lambda_c^*(1/2^-; \lambda\text{-mode}) = [[\psi_{0p}(\vec{\lambda})\psi_{0s}(\vec{\rho}), d^0]^1, \chi_c]^{1/2} D^0c, \quad (19)$$

and

$$\Lambda_c^*(3/2^-; \lambda\text{-mode}) = [[\psi_{0p}(\vec{\lambda})\psi_{0s}(\vec{\rho}), d^0]^1, \chi_c]^{3/2} D^0c. \quad (20)$$

Another possibility to construct the negative parity excited states for  $\Lambda_c^*$  is the so-called  $\rho$ -mode excitation ( $n_\rho = 0$ ,  $\ell_\rho = 1$ ), which must have the spin-1 diquark ( $d^1$ ) due to the antisymmetrization of the wave function. The total spin  $j$  of the light component can be  $j = 0, 1$  and  $2$ , leading to a HQS singlet with the baryon spin  $J = 1/2$ , and two HQS doublets  $J = (1/2, 3/2)$  and  $J = (3/2, 5/2)$ , respectively. For example, the concrete form for the HQS singlet is given by

TABLE I. Quark configurations considered in this article.  $(n_{\lambda(\rho)}, \ell_{\lambda(\rho)})$  are the nodal and the angular momentum quantum numbers for the  $\lambda(\rho)$ -motion wave function. The spin wave function of the two light quarks is expressed by  $d$ . The spin and the parity of the light component is expressed by  $j^P$ . The total angular momentum  $\vec{\ell} = \vec{\ell}_\lambda + \vec{\ell}_\rho$  are also shown for the  $\lambda\rho$ -mode. The spin and parity  $J^P$  and supposed physical charmed baryons are also shown.

Ground state charmed baryons						
$(n_\lambda, \ell_\lambda)$	$(n_\rho, \ell_\rho)$	$d^s$	$j^P$	$J^P$	Possible assignment	
(0,0)	(0,0)	$d^0$	$0^+$	$1/2^+$	$\Lambda_c(2286)$	
(0,0)	(0,0)	$d^1$	$1^+$	$(1/2, 3/2)^+$	$\Sigma_c(2455), \Sigma_c^*(2520)$	
Negative parity excited charmed baryons						
$(n_\lambda, \ell_\lambda)$	$(n_\rho, \ell_\rho)$	$d^s$	$j^P$	$J^P$	possible assignment	
(0,1)	(0,0)	$d^0$	$1^-$	$(1/2, 3/2)^-$	$\Lambda_c^*(2595), \Lambda_c^*(2625)$	
(0,0)	(0,1)	$d^1$	$0^-$	$1/2^-$		
			$1^-$	$(1/2, 3/2)^-$		
			$2^-$	$(3/2, 5/2)^-$	$\Lambda_c^*(2880)(?)$	
Positive parity excited charmed baryons						
$(n_\lambda, \ell_\lambda)$	$(n_\rho, \ell_\rho)$	$d^s$	$j^P$	$J^P$	possible assignment	
(1,0)	(0,0)	$d^0$	$0^+$	$1/2^+$		
(0,2)	(0,0)	$d^0$	$2^+$	$(3/2, 5/2)^+$	$\Lambda_c^*(2880)(?)$	
(0,0)	(1,0)	$d^0$	$0^+$	$1/2^+$		
(0,0)	(0,2)	$d^0$	$2^+$	$(3/2, 5/2)^+$	$\Lambda_c^*(2880)(?)$	
Positive parity excited charmed baryons ( $\lambda\rho$ -mode)						
$(n_\lambda, \ell_\lambda)$	$(n_\rho, \ell_\rho)$	$d^s$	$\ell$	$j^P$	$J^P$	possible assignment
(0,1)	(0,1)	$d^1$	0	$1^+$	$(1/2, 3/2)^+$	
			1	$0^+$	$1/2^+$	
				$1^+$	$(1/2, 3/2)^+$	
				$2^+$	$(3/2, 5/2)^+$	$\Lambda_c^*(2880)(?)$
		2	1	$1^+$	$(1/2, 3/2)^+$	
				$2^+$	$(3/2, 5/2)^+$	$\Lambda_c^*(2880)(?)$
				$3^+$	$(5/2, 7/2)^+$	$\Lambda_c^*(2880)(?)$

$$\Lambda_c^*(J^-; \rho\text{-mode}) = [[\psi_{0s}(\vec{\lambda})\psi_{0\rho}(\vec{\rho}), d^1]^j, \chi_c]^J = j \pm 1/2 D^0 c. \quad (21)$$

The minimal configuration for  $J^P = 1/2^+$  state for  $\Lambda_c$  baryons is an orbital excitation for the nodal quantum number  $n_\lambda = 1$  or  $n_\rho = 1$  as with the spin-0 diquark given by

$$\Lambda_c^*(1/2^+; n_\lambda = 1) = [[\psi_{1s}(\vec{\lambda})\psi_{0s}(\vec{\rho}), d^0]^0, \chi_c]^{1/2}, \quad (22)$$

$$\Lambda_c^*(1/2^+; n_\rho = 1) = [[\psi_{0s}(\vec{\lambda})\psi_{1s}(\vec{\rho}), d^0]^0, \chi_c]^{1/2}, \quad (23)$$

both of which are the HQS singlets.

The higher excited states of  $J^P$  with  $P = +$  can be constructed by the  $d$ -wave excitation as the total angular

momentum. In this case, we have three possibilities, as  $(\ell_\lambda, \ell_\rho) = (2, 0), (1, 1),$  and  $(0, 2)$ . In the  $(2, 0)$  and  $(0, 2)$  cases, the diquark spin should be 0, and the total baryon spin can be  $J = 3/2, 5/2,$  as

$$\Lambda_c^*(J^+; \ell_\lambda = 2) = [[\psi_{0d}(\vec{\lambda})\psi_{0s}(\vec{\rho}), d^0]^2, \chi_c]^{J=2 \pm 1/2} D^0 c, \quad (24)$$

$$\Lambda_c^*(J^+; \ell_\rho = 2) = [[\psi_{0s}(\vec{\lambda})\psi_{0d}(\vec{\rho}), d^0]^2, \chi_c]^{J=2 \pm 1/2} D^0 c. \quad (25)$$

In the case with  $(\ell_\lambda, \ell_\rho) = (1, 1)$ , the diquark spin should be 1, as

$$\Lambda_c^*(J^+; \ell_\lambda = 1, \ell_\rho = 1) = [[\psi_{0\rho}(\vec{\lambda})\psi_{0\rho}(\vec{\rho}), d^1]^j, \chi_c]^J D^0 c. \quad (26)$$

The total angular momentum  $\ell$  ( $\vec{\ell} = \vec{\ell}_\lambda + \vec{\ell}_\rho$ ) can be 0, 1, or 2, and the resulting light-component spin can be  $j = (1), (0, 1, 2),$  and  $(1, 2, 3),$  giving 13 states. The heavy baryons are the HQS singlet only for  $j = 0$  and the HQS doublet for the others.

We leave a comment on the difference between the wave function used in Ref. [31] and ours. In Ref. [31], the bases of the quark wave function are given by  ${}^{2s+1}\ell_j$ , namely

$$[[\ell_\lambda \ell_\rho]^\ell [[s_1 s_2] s_3]^s]^J, \quad (27)$$

while ours are given by

$$[[[\ell_\lambda \ell_\rho]^\ell [s_1 s_2]^{s_{12}}]^j s_3]^J. \quad (28)$$

They are different in general except for the highest weight state of  $\ell$  and  $s$ . In the latter, the subcomponent  $[[\ell_\lambda \ell_\rho]^\ell [s_1 s_2]^{s_{12}}]^j$ , which is assigned as the light-component spin  $j$ , decouples from the heavy quark spin  $s_3$  in the heavy quark limit. Hence the latter basis is compatible with the heavy quark symmetry.

### III. FORMULATION

#### A. Basic interaction of the pion

In the constituent quark model, the pion can couple to a single quark through the Yukawa interaction, which is considered to contribute dominantly to one-pion emission decays (Fig. 3). In the relativistic description, there are two independent couplings of pseudoscalar and axial-vector types,

$$\bar{q}\gamma_5\vec{\tau}q \cdot \vec{\pi}, \quad \bar{q}\gamma_\mu\gamma_5\vec{\tau}q \cdot \partial^\mu\vec{\pi}. \quad (29)$$

In the nonrelativistic model, they correspond to the following two terms,

$$\vec{\sigma} \cdot (\vec{p}_i - \vec{p}_f) = \vec{\sigma} \cdot \vec{q}, \quad \vec{\sigma} \cdot (\vec{p}_i + \vec{p}_f), \quad (30)$$

where  $\vec{p}_i$  ( $\vec{p}_f$ ) is the momentum of the initial (final) quarks and  $\vec{q}$  is the pion momentum. We keep in mind that these two couplings in Eq. (29) are equivalent for the on-shell particles in the initial and final states, but not for the off-shell particles confined within a finite size. The present case is the latter, because the quarks are confined in the harmonic oscillator potential. In this work, we employ the axial-vector-type coupling,

$$\mathcal{L}_{\pi qq}(x) = \frac{g_A^q}{2f_\pi} \bar{q}(x) \gamma_\mu \gamma_5 \vec{\tau} q(x) \cdot \partial^\mu \vec{\pi}(x), \quad (31)$$

in accordance with the low-energy chiral dynamics. The nonrelativistic limit in Eq. (31) leads to the combination of the two terms in Eq. (29). In Eq. (31),  $g_A^q$  is the axial coupling of the light quarks, for which we use the value  $g_A^q = 1$  [41,42]. As we will see later, importantly, the axial-vector coupling can explain surprisingly well the decay of  $\Lambda_c^*(2595)$  through the time-derivative piece in Eq. (31). On the contrary, the pseudoscalar coupling cannot reproduce it because it is proportional to the pion momentum  $q$  which almost vanishes. This strongly supports the chiral dynamics of the pion working with constituent light quarks.

### B. Matrix elements with the quark model wave functions

In this section, we formulate the one-pion emission decay of a charmed baryon within the quark model. The relevant diagram is shown in Fig. 3, where one pion is emitted from a single light quark. We write the state vector for the  $Y_c$  baryon ( $Y_c = \Lambda_c$  or  $\Sigma_c$ ) with mass  $M_{Y_c}$ , spin  $J$ , and momentum  $P$  in the baryon rest frame in the momentum representation as

$$\begin{aligned} |Y_c(P, J)\rangle &= \sqrt{2M_{Y_c}} \sum_{\{s, \ell\}} \int \frac{d^3 p_\rho}{(2\pi)^3} \int \frac{d^3 p_\lambda}{(2\pi)^3} \\ &\times \frac{1}{\sqrt{2m}} \frac{1}{\sqrt{2m}} \frac{1}{\sqrt{2M}} \psi_{\ell_\rho}(\vec{p}_\rho) \psi_{\ell_\lambda}(\vec{p}_\lambda) \\ &\times |q_1(p_1, s_1)\rangle |q_2(p_2, s_2)\rangle |q_3(p_3, s_3)\rangle, \end{aligned} \quad (32)$$

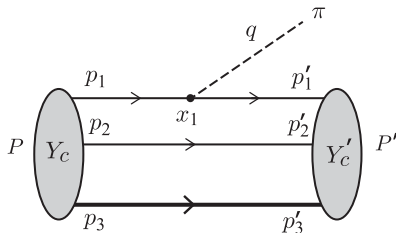


FIG. 3. Decay amplitude of the charmed baryon  $Y_c$  to  $Y'_c$  with one-pion emission.

which is a superposition of quarks in the momentum space  $|q_1(p_1, s_1)\rangle$ ,  $|q_2(p_2, s_2)\rangle$ , and  $|q_3(p_3, s_3)\rangle$ , weighted by the baryon wave functions  $\psi_\rho(\vec{p}_\rho)$  and  $\psi_\lambda(\vec{p}_\lambda)$ . Here the relative momenta  $\vec{p}_\rho$  and  $\vec{p}_\lambda$  are defined by

$$\vec{p}_\lambda = \frac{1}{2m + M} (M\vec{p}_1 + M\vec{p}_2 - 2m\vec{p}_3), \quad (33)$$

$$\vec{p}_\rho = \frac{1}{2} (\vec{p}_1 - \vec{p}_2), \quad (34)$$

and the total momentum of three quarks, which is the baryon momentum, is given by

$$\vec{P} = \vec{p}_1 + \vec{p}_2 + \vec{p}_3. \quad (35)$$

The factors of  $1/\sqrt{2m}$  are for the normalizations of the confined quark states so that  $\int \frac{d^3 p_j}{(2\pi)^3} |\psi(\vec{p}_j)|^2 = 1$ . The sum  $\sum_{\{s, \ell\}}$  is taken over the spins of the three quarks and their angular momenta such that the total angular momentum gives the spin  $J$ .

The decay amplitude for  $Y_c \rightarrow Y'_c \pi$  is given by

$$\int d^4 x_1 \langle Y'_c(P', J') \pi(q) | i\mathcal{L}(x_1) | Y_c(P, J) \rangle, \quad (36)$$

where only one light quark  $|q_1\rangle$  in the initial and final baryon state participates in the transition as

$$\begin{aligned} &\langle q'_1(p'_1, s'_1) \pi(q) | i\mathcal{L}_{\pi qq}(x_1) | q_1(p_1, s_1) \rangle \\ &\simeq i \frac{g_A^q}{2f_\pi} e^{i(p'_1 - p_1 + q) \cdot x_1} \{ i\omega_\pi \langle \chi_{s'_1} | (\vec{p}_1 + \vec{p}'_1) \cdot \vec{\sigma} | \chi_{s_1} \rangle \\ &\quad - i2m \langle \chi_{s'_1} | (\vec{p}_1 - \vec{p}'_1) \cdot \vec{\sigma} | \chi_{s_1} \rangle \}, \end{aligned} \quad (37)$$

while the other light quark  $|q_2\rangle$  and the charm quark  $|q_3\rangle$  are spectators and then their matrix elements are just delta functions of their three-momenta

$$\begin{aligned} \langle q'_j(p'_j, s'_j) | q_j(p_j, s_j) \rangle &= 2E_j (2\pi)^3 \delta^{(3)}(\vec{p}'_j - \vec{p}_j) \delta_{s'_j s_j} \\ &= 2E_j \int d^3 x_j e^{-i(\vec{p}'_j - \vec{p}_j) \cdot \vec{x}_j} \langle \chi_{s'_j} | \chi_{s_j} \rangle, \end{aligned} \quad (38)$$

where  $j = 2$  or  $3$ . We have now ten  $x$ -integrals as

$$\int dx_1^0 d^3 x_1 d^3 x_2 d^3 x_3 e^{i(p'_1 - p_1 + q) \cdot x_1} e^{-i(\vec{p}'_2 - \vec{p}_2) \cdot \vec{x}_2} e^{-i(\vec{p}'_3 - \vec{p}_3) \cdot \vec{x}_3}, \quad (39)$$

and the first  $x_1^0$ -integral leads to the energy conservation  $(2\pi)\delta(E_1 - E'_1 - \omega_\pi)$  in the  $q_1 \rightarrow q'_1 \pi$  process. We rewrite the remaining  $\vec{x}$ -integrals in terms of the Jacobi coordinates and we find

$$\int d^3 X d^3 \rho d^3 \lambda e^{-i(\vec{P}' - \vec{P}) \cdot \vec{X}} e^{-i(\vec{p}' - \vec{p}_\rho) \cdot \vec{\rho}} e^{-i(\vec{p}'_\lambda - \vec{p}_\lambda) \cdot \vec{\lambda}} e^{-i\vec{q} \cdot (\vec{X} + \frac{M}{2m+M} \vec{\lambda} + \frac{1}{2} \vec{\rho})}. \quad (40)$$

The  $\vec{X}$ -integral leads to the total three-momentum conservation, via  $(2\pi)^3 \delta^{(3)}(\vec{P} - \vec{P}' - \vec{q})$ . By eliminating the common delta functions for the energy-momentum conservation, we find the amplitude for  $Y_c \rightarrow Y'_c \pi$  decay as

$$\begin{aligned} -it_{Y_c \rightarrow Y'_c \pi} &= \sum_{\{\Lambda, \Sigma\}} i \frac{g_A^q}{2f_\pi} \sqrt{2M_{Y_c}} \sqrt{2M_{Y'_c}} \frac{1}{2m} \int \frac{d^3 p_\rho}{(2\pi)^3} \int \frac{d^3 p'_\rho}{(2\pi)^3} \int \frac{d^3 p_\lambda}{(2\pi)^3} \int \frac{d^3 p'_\lambda}{(2\pi)^3} \int d^3 \lambda \\ &\times \int d^3 \rho \psi_{\ell'_\rho}^*(\vec{p}'_\rho) e^{-i\vec{p}'_\rho \cdot \vec{\rho}} \psi_{\ell_\rho}(\vec{p}_\rho) e^{i\vec{p}_\rho \cdot \vec{\rho}} \psi_{\ell'_\lambda}^*(\vec{p}'_\lambda) e^{-i\vec{p}'_\lambda \cdot \vec{\lambda}} \psi_{\ell_\lambda}(\vec{p}_\lambda) e^{i\vec{p}_\lambda \cdot \vec{\lambda}} e^{-i\vec{q}_\lambda \cdot \vec{\lambda}} e^{-i\vec{q}_\rho \cdot \vec{\rho}} \\ &\times \left\{ i\omega_\pi \langle \chi_{s'_1} | (\vec{p}'_\lambda + 2\vec{p}'_\rho) \cdot \vec{\sigma} | \chi_{s_1} \rangle + i \left( \omega_\pi \frac{M}{2m+M} - 2m \right) \langle \chi_{s'_1} | \vec{\sigma} \cdot \vec{q} | \chi_{s_1} \rangle \right\} \langle \chi_{s'_2} | \chi_{s_2} \rangle \langle \chi_{s'_c} | \chi_{s_c} \rangle, \end{aligned} \quad (41)$$

where the effective momentum transfer  $\vec{q}_\lambda$  and  $\vec{q}_\rho$  appearing in the pion plane wave  $e^{-i\vec{q} \cdot \vec{x}_1}$  is defined by

$$\vec{q}_\lambda = \frac{M}{2m+M} \vec{q}, \quad \vec{q}_\rho = \frac{1}{2} \vec{q}. \quad (42)$$

The first term in Eq. (41) involves the relative momenta  $\vec{p}'_\rho$  and  $\vec{p}'_\lambda$  of the constituent quarks in the final baryon, which can be replaced by the derivative of the wave functions as

$$\int \frac{d^3 p'_\rho}{(2\pi)^3} \vec{p}'_\rho \psi_{\ell'_\rho}^*(\vec{p}'_\rho) e^{-i\vec{p}'_\rho \cdot \vec{\rho}} = i \vec{\nabla}_\rho \int \frac{d^3 p'_\rho}{(2\pi)^3} \psi_{\ell'_\rho}^*(\vec{p}'_\rho) e^{-i\vec{p}'_\rho \cdot \vec{\rho}} = i \vec{\nabla}_\rho \psi_{\ell'_\rho}^*(\vec{\rho}), \quad (43)$$

and the same for  $\vec{p}'_\lambda$ . In the case of  $\Lambda_c(JM)^+ \rightarrow \Sigma_c(J'M')^{++} \pi^-$ , after performing the momentum integrals and by showing the flavor (isospin) part explicitly, the decay amplitude is given by

$$\begin{aligned} -it_{\Lambda_c^+ \rightarrow \Sigma_c^{++} \pi^-} &= -\frac{g_A^q}{2f_\pi} \sqrt{2M_{\Lambda_c}} \sqrt{2M_{\Sigma_c}} \frac{1}{2m} \int d^3 \lambda d^3 \rho e^{-i\vec{q}_\lambda \cdot \vec{\lambda}} e^{-i\vec{q}_\rho \cdot \vec{\rho}} \langle D^1 c | \tau_{(1)}^+ | D^0 c \rangle \langle [[\psi_{\ell_\lambda}(\lambda) \psi_{\ell_\rho}(\rho), d]^j, \chi_c]_{M'}^j | \\ &\times \left\{ \omega_\pi (i \overleftarrow{\nabla}_\lambda + 2i \overleftarrow{\nabla}_\rho) \cdot \vec{\sigma}_{(1)} + \left( \omega_\pi \frac{M}{2m+M} - 2m \right) \vec{\sigma}_{(1)} \cdot \vec{q} \right\} \langle [[\psi_{\ell_\lambda}(\lambda) \psi_{\ell_\rho}(\rho), d]^j, \chi_c]_{M'}^j \rangle, \end{aligned} \quad (44)$$

where  $\vec{\sigma}_{(1)}$  and  $\tau_{(1)}^+$  matrices operate the spin and isospin wave functions of quark 1. For simplicity, the notation for the bra and ket states

$$\begin{aligned} &| [[\psi_{\ell_\lambda}(\lambda) \psi_{\ell_\rho}(\rho), d]^j, \chi_c]_{M'}^j \rangle \\ &\equiv \sum_{\{\ell, s\}} \psi_{\ell_\lambda}(\lambda) \psi_{\ell_\rho}(\rho) | \chi_{s_1} \rangle | \chi_{s_2} \rangle | \chi_{s_c} \rangle, \end{aligned} \quad (45)$$

are used in Eq. (44). The derivatives  $\overleftarrow{\nabla}_\lambda$  and  $\overleftarrow{\nabla}_\rho$  operate the final state wave functions. We also have to consider the case that the pion couples to the another light quark  $q_2(x_2)$ . Summing over the amplitudes of the two cases coherently, we obtain the total decay amplitude.

### C. Decay widths with the helicity amplitude

The decay width of  $B_i \rightarrow B_f \pi$  is given by

$$\Gamma = \frac{1}{16\pi^2} \frac{q}{2M_i^2} \int d\Omega \sum_f |t_{B_i \rightarrow B_f \pi}|^2, \quad (46)$$

where  $q$  is the magnitude of the three-momentum of the final pion in the center-of-mass frame, and the sum is taken over the possible quantum numbers, in the present case, the spin state (helicity) of the final baryon for a given initial baryon spin. The matrix element depends on the decay angle  $\Omega$  (the angle between the quantization axis of the initial baryon spin and the momentum vector  $\vec{p}_f$  of the final baryon) and on the helicity of  $B_f$ . In this article, we employ the helicity amplitude approach to calculate the decay width in Eq. (46).

In this approach, we expand the initial spin state  $|B_i(J, J_z = J)\rangle_{z'}$ , which is quantized along a fixed  $\hat{e}_{z'}$  axis, in the angular momentum basis quantized along the direction of the momentum of the final baryon,  $\hat{e}_z = \vec{p}_f / |\vec{p}_f|$ , by

$$|B_i(J, J)\rangle_{z'} = \sum_M |B_i(J, M)\rangle_z D_{MJ}^J(-\phi, \theta, \phi), \quad (47)$$

where  $D_{MJ}^J$  are the Wigner's  $D$  functions [43]. If the spin of the final state  $\langle B_f(\vec{p}_f, h) |$  is quantized along  $\hat{e}_z$ , then the

helicity  $h$  is equal to the third component of the final state spin,

$$\langle B_f(\vec{p}_f, h) | = {}_z \langle B_f(\vec{p}_f, J', h) |, \quad (48)$$

where  $J'$  is the spin of the final baryon  $B_f$ .

Hence the matrix element is written with its angular dependence shown explicitly as

$$\begin{aligned} & {}_z \langle B_f(\vec{p}_f, J', h) \pi(-\vec{p}_f) | \hat{t} | B_i(J, J) \rangle_z \\ &= D_{MJ}^J(-\phi, \theta, \phi) {}_z \langle B_f(\vec{p}_f, J', h) \pi(-\vec{p}_f) | \hat{t} | B_i(J, h) \rangle_z, \end{aligned} \quad (49)$$

where only the diagonal element  $M = h$  remains after summing over  $\sum_M$ , because of the helicity (spin  $z$ -component) conservation. In Eq. (49) both of the initial and final spins are quantized along the  $\hat{e}_z$  axis.

Now, the helicity amplitude  $A_h$  is defined by

$$(2\pi)^4 \delta^{(4)}(P_f - P_i) A_h = {}_z \langle B_f(\vec{p}_f, J', h) \pi(-\vec{p}_f) | \hat{t} | B_i(J, h) \rangle_z. \quad (50)$$

The amplitude  $A_h$  depends on  $J$ ,  $J'$ , and  $h$ , but does not depend on the decay angle, because the spin quantization axis is chosen along the direction of the momentum of the final baryon  $\vec{p}_f$ , which is equal to the situation of the decay into the  $z$  direction. The possible angular dependence of  $\vec{p}_f$  is taken care of by the  $D$  function, and the angular-integral  $d\Omega$  in Eq. (46) then can be performed exactly and finally we find

$$\Gamma = \frac{1}{4\pi} \frac{q}{2M_i^2} \frac{1}{2J+1} \sum_h |A_h|^2, \quad (51)$$

where  $q = |\vec{p}_f|$ . Here, the amplitude  $A_{-h}$  with the opposite helicity has the same form as  $A_h$ .

#### D. Parameters

In the present Hamiltonian of the harmonic oscillator in Eq. (1), we have three model parameters;  $m$  the mass of the light quark,  $M$  that of the heavy quark, and  $k$  the spring constant. The masses of the quarks are set to be

$$\begin{aligned} m &= 0.35 \pm 0.05 \text{ (GeV)}, \\ M &= 1.5 \pm 0.1 \text{ (GeV)}. \end{aligned} \quad (52)$$

We tune the value of  $k$  so that the level spacing of the  $\lambda$ -mode excitation as  $\omega_\lambda \sim 0.35 \pm 0.05$  GeV and the root-mean-square radius of the charmed baryon as  $\sqrt{\langle R^2 \rangle} \sim 0.45\text{--}0.55$  fm, which is defined as the average of the distance of each quark from the center of mass as

TABLE II. Range of the model parameters of  $\{m, M, k\}$  (inputs) and the properties of resulting harmonic oscillator (H.O.) functions (outputs).

Inputs		
	light quark mass $m$	0.3–0.4 (GeV)
	heavy quark mass $M$	1.4–1.6 (GeV)
	H.O. potential $k$	0.02–0.038 (GeV <sup>3</sup> )
	H.O. energy $\omega_\lambda$	0.3–0.4 (GeV)
Outputs	H.O. energy $\omega_\rho$	0.42–0.58 (GeV)
	Gauss range $a_\lambda$	0.36–0.44 (GeV)
	Gauss range $a_\rho$	0.26–0.32 (GeV)
	$\sqrt{\langle \lambda^2 \rangle}$	0.55–0.67 (fm)
	$\sqrt{\langle \rho^2 \rangle}$	0.76–0.93 (fm)
	$\sqrt{\langle R^2 \rangle}$	0.45–0.55 (fm)

$$\begin{aligned} R^2 &\equiv \frac{1}{3} \sum_{i=1}^3 (\vec{r}_i - \vec{X})^2 \\ &= \frac{1}{3} \left( \frac{2(2m^2 + M^2)}{(2m + M)^2} \lambda^2 + \frac{1}{2} \rho^2 \right). \end{aligned} \quad (53)$$

We summarize the model parameters used in the present calculation in Table II. Depending on these input parameters, the range parameters of the Gaussian wave functions vary within the range of

$$\begin{aligned} a_\lambda &= 0.36\text{--}0.44 \text{ (GeV)}, \\ a_\rho &= 0.26\text{--}0.32 \text{ (GeV)}, \end{aligned} \quad (54)$$

which is the source of the uncertainty in our theory predictions.

### III. NUMERICAL RESULTS

#### A. Decays of the ground state $\Sigma_c(1/2^+)$ and $\Sigma_c^*(3/2^+) \rightarrow \Lambda_c(1/2^+) \pi$

The  $\Sigma_c(2455)$  baryon is an orbital ground state baryon having  $J^P = 1/2^+$ . The mass of the  $\Sigma_c(2455)^{++}$  is  $2453.97 \pm 0.14$  MeV and its full width is  $1.89_{-0.18}^{+0.09}$  (MeV) [24]. The  $\Sigma_c(2455) \rightarrow \Lambda_c(2286)\pi$  decay channel is the only possible strong decay and its branching ratio is  $\sim 100\%$ . The  $\Sigma_c^*(2520)$  baryon has  $J^P = 3/2^+$  and is expected to form a HQS doublet with  $\Sigma_c(2455)$ . The mass of the  $\Sigma_c^*(2520)^{++}$  is  $2518.41_{-0.19}^{+0.21}$  (MeV) and its width is  $14.78_{-0.40}^{+0.30}$  (MeV) [24]. Again the  $\Lambda_c(2286)\pi$  decay channel is the only possible channel in the strong decay and its branching ratio is  $\sim 100\%$ . Because both  $\Sigma_c(2455)$  and  $\Sigma_c^*(2520)$  baryons are the spin and isospin flip states of the ground state  $\Lambda_c(2286)$ , their decay rates reflect mainly the spin-isospin structure and is rather insensitive to the spatial structure. Therefore, we can use these processes to check the validity of the present quark model calculations.

The helicity amplitude for the  $\Sigma_c(1/2^+) \rightarrow \Lambda_c(1/2^+)\pi$  decay is given by

$$A_h = A_h^{\nabla\cdot\sigma} + A_h^{q\cdot\sigma}, \quad (55)$$

where  $A_h^{\nabla\cdot\sigma}$  and  $A_h^{q\cdot\sigma}$  correspond to the  $(\vec{\nabla}_\lambda + 2\vec{\nabla}_\rho) \cdot \vec{\sigma}$  term and the  $\vec{q} \cdot \vec{\sigma}$  term in Eq. (44), respectively. They are given by

$$-iA_{1/2}^{\nabla\cdot\sigma} = G \frac{\omega_\pi}{m} \left( -\frac{1}{\sqrt{3}} \right) \left( \frac{1}{2} q_\lambda + q_\rho \right) F(q), \quad (56)$$

and

$$-iA_{1/2}^{q\cdot\sigma} = -G \frac{q}{m} \left( -\frac{1}{\sqrt{3}} \right) \left( \frac{M}{2m+M} \omega_\pi - 2m \right) F(q), \quad (57)$$

where  $q_{\lambda(\rho)} \equiv |\vec{q}_{\lambda(\rho)}|$  and  $G$  denotes the coupling constant and the normalizations as

$$G = \frac{g_A^q}{2f_\pi} \sqrt{2M_{\Lambda_c}} \sqrt{2M_{\Sigma_c}}. \quad (58)$$

The function  $F(q)$  denotes the Gaussian form factor as

$$F(q) = e^{-q_\lambda^2/4a_\lambda^2} e^{-q_\rho^2/4a_\rho^2}, \quad (59)$$

which is the Fourier transform of ground to ground transition amplitude. The factors of  $a_\lambda$  and  $a_\rho$  correspond to the inverse of the range of the Gaussian wave functions for  $\lambda$ - and  $\rho$ -motions, respectively, and their definitions are given in Appendix A. Similarly, the helicity amplitude for the  $\Sigma_c^*(3/2^+) \rightarrow \Lambda_c(1/2^+)\pi$  decay is given by the same expressions as Eqs. (56) and (57) but the factor  $-1/\sqrt{3}$  is replaced by  $\sqrt{2/3}$  in both equations.

In Table III, we show the numerical results for the  $\Sigma_c(2455)(1/2^+) \rightarrow \Lambda_c^+\pi^+$  decay. The calculated decay width is almost twice as large as the experimental value. We also show the results of the  $\Sigma_c^*(2520)(3/2^+)$  decay in the same table. The calculated decay width of  $\Sigma_c^*(3/2^+)$  is again twice as large as the experimental value.

TABLE III. Calculated decay widths of  $\Sigma_c(2455)^{++}$  and  $\Sigma_c^*(2520)^{++}$  into the  $\Lambda_c(2286)^+\pi^+$  pair.  $q$  is the momentum of the final particle in the center-of-mass frame.

$B_i J^P$ (MeV)	$\Gamma_{\text{exp}}$ (MeV)	$q$ (MeV/c)	$\Gamma_{\text{th}}(\Sigma_c(J^+)^{++} \rightarrow \Lambda_c(2286)^+\pi^+)$ (MeV)
$\Sigma_c(2455)^{++} 1/2^+$ (2453.98)	1.89	89	4.27–4.33
$\Sigma_c^*(2520)^{++} 3/2^+$ (2517.9)	14.78	177	30.3–31.6

As shown in the table, the uncertainty from the ambiguities of the quark model parameters ( $m, M, k$ ) is small, which means the decay width of the ground state to the ground state does not depend on the detail of the wave functions, as anticipated. Therefore the discrepancy might come from the axial-coupling constant  $g_A^q$  for the  $\pi q q$  interaction.

In the present calculation, we employ  $g_A^q = 1$  for the  $q\pi\pi$  coupling, but it is also known that this value does not reproduce the axial-coupling constant of the nucleon  $g_A^N = 1.25$  but leads to  $g_A^N = 5/3$  instead. To reproduce the axial-coupling constant of the nucleon  $g_A^N$ , one needs a suppression factor of about 3/4 for  $g_A^q$ , which reduces the decay width by a factor  $(3/4)^2 \sim 0.56$ , the result of which is consistent with the experimental data. This is expected because the pion emission decays essentially measure the axial couplings for the relevant baryons (transitions). Our input here is the axial coupling of the constituent quarks, which can take in principle any value when chiral symmetry is spontaneously broken. Here we have shown that it is about 3/4 empirically from the phenomena of the ground state baryons not only for the nucleon but also for charmed baryons, which is not far from the discussion of Weinberg [41]. The suppression of  $g_A$  has been considered to be originated from the mixing of  $p$ -waves due to relativistic corrections or pion clouds [44]. This, however, may vary for different baryon excitations. Keeping this in mind, in the following calculations for decays of the excited states, we keep using the value  $g_A^q = 1$ .

### B. $\Lambda_c^*(2595)(1/2^-) \rightarrow \Sigma_c(2455)(1/2^+)\pi$

The  $\Lambda_c^*(2595)^+$  baryon is the first excited charmed baryons with  $I = 0$  and is expected to have  $J^P = 1/2^-$ . The total decay width is  $\Gamma_{\text{exp}} = 2.6 \pm 0.6$  MeV, where the  $\Lambda_c^+\pi\pi$  channel is the only strong decay. The  $\Lambda_c^+\pi\pi$  seems to be dominated by  $\Sigma_c(2455)\pi$  and its branching ratio  $\Gamma(\Sigma_c\pi)/\Gamma(\text{total})$  is quoted as  $\text{BR}(\Sigma_c^{++}\pi^-) = \text{BR}(\Sigma_c^0\pi^+) = (24 \pm 7)\%$  [24]. The direct three-body decay width is  $18 \pm 10\%$ , which we do not calculate in this article.

Employing the quark model, we have three possibilities to describe the excited  $\Lambda_c^*$  baryon having  $J^P = 1/2^-$  as discussed in the previous section. One is the  $\lambda$ -mode excitation having  $j^P = 1^-$ , and the other two are the  $\rho$ -mode excitations having  $j^P = 0^-$  and  $j^P = 1^-$ .

The helicity amplitude for the  $\pi^-$  emission decay of  $\Lambda_c^*(1/2^-; \lambda)^+ \rightarrow \Sigma_c(1/2^+)^{++}\pi^-$  is found again as the sum

$$A_h(1/2^-; \lambda) = A_h^{\nabla\cdot\sigma}(1/2^-; \lambda) + A_h^{q\cdot\sigma}(1/2^-; \lambda), \quad (60)$$

where

$$-iA_{1/2}^{\nabla\sigma}(1/2^-; \lambda) = iG \frac{\omega_\pi}{m} \left\{ c_0 a_\lambda + c_2 \left( \frac{1}{2} q_\lambda + q_\rho \right) \frac{q_\lambda}{a_\lambda} \right\} F(q), \quad (61)$$

and

$$-iA_{1/2}^{q\sigma}(1/2^-; \lambda) = -iG \frac{q}{m} \left( \frac{M}{2m+M} \omega_\pi - 2m \right) c_2 \frac{q_\lambda}{a_\lambda} F(q), \quad (62)$$

where

$$c_0 = -\frac{1}{\sqrt{2}}, \quad c_2 = \frac{1}{3\sqrt{2}}, \quad (63)$$

which are determined by the Clebsch-Gordan coefficients. We summarize the general expressions in Appendix B. We can see that the  $A^{\nabla\sigma}$  starts from  $\mathcal{O}(q^0)$ , reflecting properly the nature of the possible  $s$ -wave decay, while  $A^{q\sigma}$  is of order  $\mathcal{O}(q^2)$ . We will see that the former gives a considerable contribution to the  $\Lambda_c^*(2595)$  decay width.

As for the  $\rho$ -mode with  $j = 1$ , we find a similar form for the  $\Lambda_c^*(1/2^-, \rho_{j=1})^+ \rightarrow \Sigma(1/2^+)^{++} \pi^-$  decay as

$$\begin{aligned} & -iA_{1/2}^{\nabla\sigma}(1/2^-; \rho_{j=1}) \\ & = iG \frac{\omega_\pi}{m} \left\{ c_0 a_\rho + c_2 \left( \frac{1}{2} q_\lambda + q_\rho \right) \frac{q_\rho}{a_\rho} \right\} F(q), \end{aligned} \quad (64)$$

and

$$\begin{aligned} & -iA_{1/2}^{q\sigma}(1/2^-; \rho_{j=1}) \\ & = -iG \frac{q}{m} \left( \frac{M}{2m+M} \omega_\pi - 2m \right) c_2 \frac{q_\rho}{a_\rho} F(q), \end{aligned} \quad (65)$$

where

$$c_0 = 2, \quad c_2 = -\frac{1}{3}. \quad (66)$$

In contrast to the above two cases, the situation is quite different for the decay of  $\Lambda_c^*(1/2^-, \rho_{j=0})$  having the light spin  $j = 0$ . The amplitudes are exactly zero as

$$A_{1/2}^{\nabla\sigma}(1/2^-; \rho_{j=0}) = 0, \quad (67)$$

$$A_{1/2}^{q\sigma}(1/2^-; \rho_{j=0}) = 0, \quad (68)$$

for the decay into the  $\Sigma_c(1/2^+)$  baryon. This is due to the spin conservation of the light component; the spin-parity  $j^P = 0^-$  state cannot decay into  $j^P = 1^+$  with the pion  $0^-$  for any combination of relative angular momentum. Generally, as we will see in other examples, such requirements lead to selection rules due to the consistency between

the decays of baryons and decays of the light component, or the diquark in the quark model because the pion couples only to the light quarks. Such observations can be done best by using the baryon wave functions as inspired by the heavy quark symmetry.

To estimate the decay width of the  $\Lambda_c^*(2595)$  baryon, we should take the finite width of the final  $\Sigma_c$  baryon into account, because the  $\Sigma_c \pi$  threshold is very close to the  $\Lambda_c^*(2595)$  mass. Indeed, the  $\Sigma_c^+ \pi^-$  and  $\Sigma_c^0 \pi^+$  channels barely close at the  $\Lambda_c^*(2595)$  mass while the  $\Sigma_c^+ \pi^0$  channel opens, which means the isospin breaking is large contrary to the assumption made in PDG [24]. To this end, we convolute the decay width of  $\Lambda_c^*(2595)$  by the finite width of  $\Sigma_c$  as

$$\tilde{\Gamma}_{\Lambda_c^*} = \frac{1}{N} \int d\tilde{M}_{\Sigma_c} \text{Im} \frac{\Gamma_{\Lambda_c^*}(\tilde{M}_{\Sigma_c})}{\tilde{M}_{\Sigma_c} - M_{\Sigma_c} + i\Gamma_{\Sigma_c}(\tilde{M}_{\Sigma_c})/2}, \quad (69)$$

where  $\Gamma_{\Lambda_c^*}(\tilde{M}_{\Sigma_c})$  is the calculated decay width of  $\Lambda_c^*$  given in Eq. (51) which depends on the mass  $\tilde{M}_{\Sigma_c}$  of the final  $\Sigma_c$  baryon. The normalization factor  $N$  is defined by

$$N = \int d\tilde{M}_{\Sigma_c} \text{Im} \frac{1}{\tilde{M}_{\Sigma_c} - M_{\Sigma_c} + i\Gamma_{\Sigma_c}(\tilde{M}_{\Sigma_c})/2}. \quad (70)$$

We take into account the phase space factor for the  $\Sigma_c$  decay width in the convolution integral as

$$\begin{aligned} \Gamma_{\Sigma}(\tilde{M}_{\Sigma_c}) & = \Gamma_{\Sigma_c} \frac{M_{\Sigma_c}}{\tilde{M}_{\Sigma_c}} \left( \frac{\lambda^{1/2}(\tilde{M}_{\Sigma_c}^2, M_{\Lambda_c}^2, m_\pi^2)}{\lambda^{1/2}(M_{\Sigma_c}^2, M_{\Lambda_c}^2, m_\pi^2)} \right)^3 \\ & \quad \times \theta(\tilde{M}_{\Sigma_c} - M_{\Lambda_c} - m_\pi), \end{aligned} \quad (71)$$

where  $M_{\Lambda_c}$  is the mass of the ground state  $\Lambda_c(2286)$ , and  $\Gamma_{\Sigma_c}$  is the decay width of  $\Sigma_c$  given by  $\Gamma_{\Sigma_c} = 1.89$  (MeV) for  $\Sigma_c^{++}$ ,  $\Gamma_{\Sigma_c} = 1.83$  (MeV) for  $\Sigma_c^0$ . Because only the upper limit is determined for  $\Sigma_c^+$ , we calculate the ratio of  $\Gamma(\Sigma_c^{++})/\Gamma(\Sigma_c^+)$  by employing our formalism discussed in Sec. IV A, and then estimate it as  $\Gamma_{\Sigma_c} = 2.1$  (MeV) for  $\Sigma_c^+$ . The convolution corresponds to the consideration of the sequential decay of the  $\Lambda_c^* \rightarrow \Sigma_c \pi$  followed by  $\Sigma_c \rightarrow \Lambda_c \pi$  as depicted in Fig. 4. The double  $\pi^0$  emission decay of  $\Lambda_c^*(2595)^+ \rightarrow \Lambda_c(2286) \pi^0 \pi^0$  can be approximated by the convoluted single  $\pi^0$  decay of  $\Lambda_c^*(2595)^+ \rightarrow \Sigma_c(2455)^+ \pi^0$  (including a symmetry factor for the two

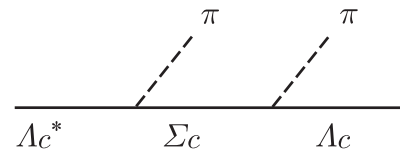


FIG. 4. Feynman diagram of the sequential decay of  $\Lambda_c^* \rightarrow \Sigma_c \pi$  followed by  $\Sigma_c \rightarrow \Lambda_c \pi$  supposed in Eq. (69).

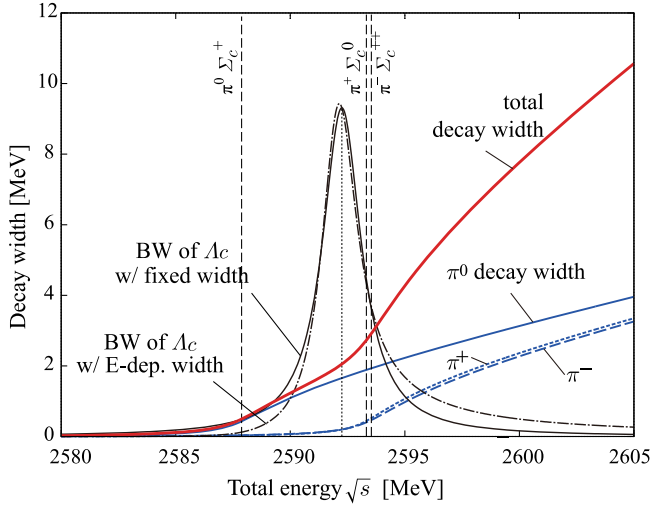


FIG. 5. Convoluted decay width of  $\Lambda_c^*(2595; \lambda\text{-mode}) \rightarrow \Sigma_c(2455)\pi$  as functions of total energy (= the mass of the  $\Lambda_c^*$ ). The thin (blue) lines denote the  $\pi^-$ ,  $\pi^0$ , and  $\pi^+$  emission decay widths as indicated in the figure. The thick (red) solid line denotes the sum of the three charge states. The resulting Breit-Wigner spectral functions of the  $\Lambda_c^*$  are also shown in arbitrary units.

identical particles), because of the dominant contribution of the on-shell  $\Sigma_c$  [27]. Similarly, the charged pion decay  $\Lambda_c \pi^+ \pi^-$  is approximated by the sum of the  $\Sigma_c^{++} \pi^-$  and  $\Sigma_c^0 \pi^+$  decays.

In Fig. 5, we show the calculated result for the decay width of the  $\Lambda_c^*(2595)$  baryon in the case of the  $\lambda$ -mode as functions of the mass of the  $\Lambda_c^*$  (the total energy  $\sqrt{s}$ ). We find that the  $\pi^\pm$  decay width remains finite even at  $\sqrt{s} = M_{\Lambda_c^*}$ , which is below the  $\pi^\pm$  threshold, owing to the finite width of the  $\Sigma_c$  baryon. We can also see that the  $\pi^0$  threshold is located at 5 MeV below  $\sqrt{s} = M_{\Lambda_c^*}$  and then the  $\pi^0$  decay width is much larger than that of  $\pi^\pm$ , meaning a large isospin breaking. We also show the resulting

Breit-Wigner (BW) form in Fig. 5 with the fixed width at  $\sqrt{s} = M_{\Lambda_c^*} = 2592.25$  (MeV) and with the energy-dependent width. In the present case, the two BW functions resemble each other because of the resulting small width. However, the energy dependence of the width is large, so we have to be careful when estimating the BW width for  $\Lambda_c^*(2595)$ .

In Table IV we show the calculated decay widths of  $\Lambda_c^*(2595)^+ \rightarrow \Sigma_c(2455)^{++} \pi^-$ ,  $\Sigma_c(2455)^0 \pi^+$ , and  $\Sigma_c(2455)^+ \pi^0$  together with the sum of these three channels evaluated at  $\sqrt{s} = M_{\Lambda_c^*} = 2592.25$  (MeV). These numbers have uncertainty reflecting that of model parameters of  $(m, M, k)$  as discussed in Sec. III D. The uncertainty of the model parameters leads to an almost factor-2 difference in the decay widths. In spite of this uncertainty, including the one coming from  $g_A^q$ , using the axial-vector coupling works well to reproduce the relatively large decay width of  $\Lambda_c^*(2595)$  located at almost the  $\Sigma_c \pi$  threshold. This is due to the time-derivative term with the strength determined by the mass of the pion. Thus the decay of  $\Lambda_c^*(2595)$  provides a good example to show that the chiral theory works up to the order  $\mathcal{O}(m_\pi)$ . As discussed in the previous section, we find that, by employing the pseudoscalar coupling ( $\gamma_5$ ) for the pion, we obtain less than 1 (keV) for the  $\Lambda_c^*(2595)$  decay due to the small pion momentum  $q$ .

We also find that the assignment of the  $\rho$ -mode configuration with  $j^P = 1^-$  to the  $\Lambda_c^*(2595)$  leads to an almost 2.5–5 times larger width than the experimental value for the total width. They are significantly large even if we consider the uncertainty of the pion coupling, because the experimental total width contains not only the  $\Sigma_c \pi$  decay channel but also the nonresonant three-body decay of  $\Lambda_c \pi \pi$ , which we do not consider in this paper.

In addition, the  $\rho$ -mode configuration with  $j^P = 0^-$  cannot decay into  $\Sigma_c \pi$ . Therefore we can conclude that, by a detailed study of decay width, it is likely that the  $\Lambda_c^*(2595)$  baryon is dominated by the  $\lambda$ -mode configuration

TABLE IV. Calculated decay width of the  $\Lambda_c^*(2595) \rightarrow \Sigma_c(2455)\pi$ . The charge decay channels are indicated in the table, where  $[\Sigma_c \pi]^+$  denotes the isospin summed width. The quantum numbers of the  $\lambda$ - and  $\rho$ -modes are indicated by  $(n_\lambda, \ell_\lambda)$  and  $(n_\rho, \ell_\rho)$ , and  $J_{\Lambda_c^*}(j)^P$  stands for the assigned spin and parity for  $\Lambda_c^*$  with the light-component spin  $j$ . The masses of  $\Lambda_c^*$ ,  $\Sigma_c$ , and  $\pi$  are also shown in the table. The symbol  $\dagger$  indicates the closed channels for on-shell  $\Sigma_c \pi$ .

$\Lambda_c^*(2595)^+$ Decay width [ $M_{\Lambda_c^*} = 2592.25$ (MeV)]						
Decay channel	full	$[\Sigma_c \pi]^+$	$\Sigma_c^{++} \pi^-$	$\Sigma_c^0 \pi^+$	$\Sigma_c^+ \pi^0$	
Experimental value $\Gamma_{\text{exp}}$ (MeV) [24]	$2.6 \pm 0.6$	...	0.624 (24%)	0.624 (24%)	...	
Momentum of final particle $q$ (MeV/c)	...	...	$\dagger$	$\dagger$	34	
This work	$(n_\lambda, \ell_\lambda), (n_\rho, \ell_\rho)$	$J_{\Lambda_c^*}(j)^P$				
$\Gamma$	(0,1), (0,0)	$1/2(1)^-$	1.5–2.9	0.13–0.25	0.15–0.28	1.2–2.4
(MeV)	(0,0), (0,1)	$1/2(0)^-$	0	0	0	0
		$1/2(1)^-$	6.5–11.9	0.57–1.04	0.63–1.15	5.3–9.7
			$M_\Sigma$ (MeV)	2453.97	2453.75	2452.9
input parameters employed			$\Gamma_\Sigma$ (MeV)	1.89	1.83	2.2
in the convolution Eq. (69)			$m_\pi$ (MeV)	139.57	139.57	134.98

as expected. We might add a comment that other assignments of the  $J^P = 3/2^-$  or higher spin configurations for  $\Lambda_c^*(2595)$  cannot reproduce the large experimental value for the decay width due to the  $d$ -wave (or higher partial wave) nature.

### C. $\Lambda_c^*(2625)(3/2^-) \rightarrow \Sigma_c(2455)(1/2^+)\pi$

The  $\Lambda_c^*(2625)^+$  baryon is a very narrow resonant state and is expected to have  $J^P = 3/2^-$ . In PDG, only the upper limit of the decay width is given as  $\Gamma_{\text{exp}} < 0.97$  MeV [24]. The  $\Lambda_c^+\pi\pi$  and its submode  $\Sigma_c\pi$  are the only strong decay channels. The branching ratio  $\text{BR}(\Sigma_c^{++}\pi^-)/\text{BR}(\Lambda_c^+\pi^+\pi^-)$  is less than 5%, and therefore the partial decay width for  $\Gamma_{\text{exp}}(\Lambda_c^*(2625)^+ \rightarrow \Sigma_c^{++}\pi^-)$  is less than 0.05 MeV.

As discussed in the previous section, the  $\Lambda_c^*(2625)$  baryon is assigned to be the low-lying orbital excitation state with  $\ell_\lambda = 1$  with a spin-0 light diquark. The helicity amplitude for the  $\Lambda_c^*(3/2^-; \lambda)^+ \rightarrow \Sigma_c^{++}\pi^-$  is then given by the same expressions as Eqs. (61) and (62) but with the different coefficients as

$$c_0 = 0, \quad c_2 = -\frac{1}{3}. \quad (72)$$

In contrast to the case of  $\Lambda_c^*(2595)$ , the coefficient  $c_0$  of the  $q^0$  term is zero and then the helicity amplitudes  $A_h^{\nabla\sigma}$  and  $A_h^{q\sigma}$  are of order of  $\mathcal{O}(q^2)$ , as expected for the  $3/2^- \rightarrow 1/2^+ + 0^-$  decay.

We have two more possible quark configurations for the  $\Lambda_c^*$  excitations with  $J^P = 3/2^-$ , which are the  $\rho$ -mode excitations with  $j = 1$  and  $j = 2$ . The helicity amplitudes for these configurations are found to be again the same as Eqs. (64) and (65) but with different coefficients as

$$c_0 = 0, \quad c_2 = -\frac{1}{3\sqrt{2}}, \quad (73)$$

for the  $\Lambda_c^*(3/2^-, \rho_{j=1}) \rightarrow \Sigma_c(1/2^+)\pi$  decay, and

$$c_0 = 0, \quad c_2 = \frac{1}{\sqrt{10}}, \quad (74)$$

for  $\Lambda_c^*(3/2^-, \rho_{j=2}) \rightarrow \Sigma_c(1/2^+)\pi$  decay.

In Table V we show the numerical results for the  $\Lambda_c^*(2625)^+ \rightarrow \Sigma_c(2455)^{++}\pi^-$  decay. In the  $\Lambda_c^*(2625)$  case, we do not convolute over the finite width of  $\Sigma_c$  because the  $\Sigma_c\pi$  threshold is well below the  $\Lambda_c^*(2625)$  mass, and the convolution does not change the result much. In the table, we also show the calculated decay widths of other assignments than  $J^P = 3/2^-$ .

We find that the assignment of the  $\lambda$ -mode configuration with  $J^P = 3/2^-$  for  $\Lambda_c^*(2625)$  works very well to describe the small decay width of  $\Lambda_c^*(2625) \rightarrow \Sigma_c\pi$ , while the assignment of  $1/2^-$  leads to a larger width than the experimental value. In contrast to the case of

TABLE V. Calculated decay widths of the  $\Lambda_c^*(2625) \rightarrow \Sigma_c(2455)^{++}\pi^-$ . The quantum numbers of the  $\lambda$ - and  $\rho$ -mode are indicated by  $(n_\lambda, \ell_\lambda)$  and  $(n_\rho, \ell_\rho)$ , and  $J_{\Lambda_c^*}(j)^P$  stands for the assigned spin and parity for  $\Lambda_c^*$  with the light-component spin  $j$ . The masses of the  $\Sigma_c^{++}$  and  $\pi^-$  are  $M_{\Sigma_c^{++}} = 2453.97$  (MeV) and  $m_{\pi^-} = 139.57$  (MeV).

$\Lambda_c^*(2625)^+$ decay width [ $M_{\Lambda_c^*} = 2628.11$ (MeV)]			
decay channel		full	$\Sigma_c^{++}\pi^-$
Experimental value $\Gamma_{\text{exp}}$ (MeV) [24]		$< 0.97$	$< 0.05 (< 5\%)$
Momentum of final particle $q$ (MeV/c)		...	101
This work	$(n_\lambda, \ell_\lambda), (n_\rho, \ell_\rho)$	$J_{\Lambda_c^*}(j)^P$	
$\Gamma$ (MeV)	(0,1), (0,0)	$1/2(1)^-$	5.4–10.7
		$3/2(1)^-$	0.024–0.039
	(0,0), (0,1)	$1/2(0)^-$	0
		$1/2(1)^-$	24.0–45.1
		$3/2(1)^-$	0.013–0.019
		$3/2(2)^-$	0.023–0.034
		$5/2(2)^-$	0.010–0.015

$\Lambda_c^*(2595)(1/2^-)$ , however, we cannot exclude the possibilities of the  $\rho$ -mode configurations for  $\Lambda_c^*(2625)(3/2^-)$  by the study of decay width, because the calculated  $\Sigma_c\pi$  decay widths for the  $\lambda$ -mode and the two  $\rho$ -modes with  $J = 3/2^-$  are accidentally similar to each other. It is interesting, however, that these three modes give quite different transition amplitudes for the  $\Sigma_c^*(3/2^+)\pi$  decay as will be discussed later in Sec. IV D, although the  $\Sigma_c^*\pi$  channel is closed for  $\Lambda_c^*(2625)$ . To discuss the structure of  $\Lambda_c^*(2625)$  in more detail, we need systematical analyses of the mass spectrum [23], nonresonant three-body decay, and so on.

### D. Decays of the higher excited $\Lambda_c^*$ baryons

In Ref. [24], three more  $\Lambda_c^*$  states are nominated,  $\Lambda_c^*(2765)$ ,  $\Lambda_c^*(2880)$ , and  $\Lambda_c^*(2940)$ , though  $\Sigma_c^*(2765)$  cannot be excluded for  $\Lambda_c^*(2765)$ . Among them, spin of  $\Lambda_c^*(2880)$  is the only quantum number that is well determined in the experiment. The parity of  $\Lambda_c^*(2880)$  is assigned to be positive, but it deserves being carefully examined. Therefore we consider possible assignments of both positive and negative parity cases. For these higher states, the  $\Sigma_c^*(2520)\pi$  channel opens in addition to the  $\Sigma_c(2450)\pi$  channel. The ratio of  $\Gamma(\Sigma_c^*\pi)/\Gamma(\Sigma_c\pi)$  also can help us to determine the quantum numbers, and the quark configuration as well. In the following discussions,  $\Sigma_c^{(*)}$  denotes  $\Sigma_c(2455)$  with  $1/2^+$  or  $\Sigma_c^*(2520)$  with  $3/2^+$ .

#### 1. $\Lambda_c^*(2765) \rightarrow \Sigma_c^{(*)}\pi$ decay

The  $\Lambda_c^*(2765)$  baryon is seen in  $\Lambda_c^+\pi^+\pi^-$  channel as a broad peak [24,45]. The width is reported as  $\Gamma_{\text{exp}} = 50$  (MeV), but its quantum numbers are still unknown. For this baryon, we consider the  $p$ -wave excitations in a  $\lambda$ - or  $\rho$ -mode with negative parity;  $\{(n_\lambda, \ell_\lambda), (n_\rho, \ell_\rho)\} = \{(0, 1), (0, 0)\}$  or  $\{(0, 0), (0, 1)\}$ .

We also consider the possibility of  $s$ -wave or  $d$ -wave excitations in  $\lambda$ -mode with positive parity;  $\{(n_\lambda, \ell_\lambda), (n_\rho, \ell_\rho)\} = \{(1, 0), (0, 0)\}$  or  $\{(0, 2), (0, 0)\}$ . Further studies on  $\Lambda_c^*(2765)$  with other quark configurations are in progress and will be discussed elsewhere [46].

In Table VI, we summarize the possible  $\Lambda_c^*$  spin-parity considered here together with the calculated results. Because the partial decay widths are not measured yet, we show the isospin summed width calculated by using the isospin-averaged masses  $M_{\Sigma_c^{(*)}}$  and  $m_\pi$ . The concrete forms of the helicity amplitudes are summarized in Appendix B. We find that, for a higher  $j$ , the decay width tends to be smaller due to the suppression of the phase space for higher relative angular momentum in the final state.

In the last column in Table VI, we also show the ratio of the decay widths to  $\Sigma_c(2455)\pi$  and  $\Sigma_c^*(2520)\pi$  defined by

$$R = \frac{\Gamma(\Lambda_c^* \rightarrow \Sigma_c^* \pi)}{\Gamma(\Lambda_c^* \rightarrow \Sigma_c \pi)}. \quad (75)$$

We find the order of magnitudes of the ratio  $R$  are quite different for different configurations even if the spin-parity is the same, e.g.  $J_{\Lambda_c^*}(j)^P = 3/2(1)^-(\lambda\text{-mode})$ ,  $3/2(1)^-(\rho\text{-mode})$ , and  $3/2(2)^-(\rho\text{-mode})$ . In fact, these three modes give similar widths for the  $\Sigma_c \pi$  decay as discussed in the previous section, but give quite different widths for  $\Sigma_c^* \pi$ . In principle, the  $\Lambda_c^*(3/2^-)$  baryon can decay by  $s$ -wave to  $\Sigma_c^*(3/2^+)\pi(0^-)$ , while it decays by  $d$ -wave to  $\Sigma_c(1/2^+)\pi(0^-)$ . Then the ratio  $R$  can be expressed by

$$R = \frac{\Gamma(\Sigma_c^* \pi)_s + \Gamma(\Sigma_c^* \pi)_d}{\Gamma(\Sigma_c \pi)_d}, \quad (76)$$

which is, in general, larger than unity. This is the case for the  $J_{\Lambda_c^*}(j)^P = 3/2(1)^-$  as

$$R(3/2(1)^-(\lambda\text{-mode})) = 5.6\text{--}7.8, \quad (77)$$

$$R(3/2(1)^-(\rho\text{-mode})) = 49\text{--}70. \quad (78)$$

In contrast, the light quark system having  $j^P = 2^-$  cannot decay by  $s$ -wave to that of  $1^+$  in  $\Sigma_c^*(3/2^+)\pi(0^-)$  because of the spin-parity conservation. This is another example of the selection rules in the heavy quark limit. Due to the absence of an  $s$ -wave contribution, the ratio  $R$  is smaller than unity for  $3/2(2)^-$  as

$$R(3/2(2)^-(\rho\text{-mode})) = \frac{\Gamma(\Sigma_c^* \pi)_d}{\Gamma(\Sigma_c \pi)_d} = 0.25\text{--}0.26. \quad (79)$$

In this configuration, the amplitudes of  $\Sigma_c \pi$  and  $\Sigma_c^* \pi$  decays are the same except the momentum  $q$  of pion as discussed in Ref. [3]. Here, we stress that the  $s$ -wave suppression for  $J_{\Lambda_c^*}^P = 3/2^-$  is found only in the case of  $j^P = 2^-$ , and not in the other quark configurations. This is the same phenomenon that the  $1/2(0)^-$  state cannot decay into  $\Sigma_c^{(*)} \pi$  as mentioned in Sec. IV B, and also is seen for the decay of the  $\Lambda_c^*(2880)$  as discussed in the next section.

As for the magnitude of the decay width, we find that the assignments of  $J_{\Lambda_c^*}(j)^P = 1/2(1)^-$  and  $3/2(1)^-$  ( $\ell_\rho = 1$ ) give rather large decay widths due to the  $s$ -wave nature into either  $\Sigma_c(1/2^+)\pi$  or  $\Sigma_c^*(3/2^+)\pi$ . We can exclude these assignments because the resulting decay widths are too large. Calculated widths for  $\lambda$ -modes ( $\ell_\lambda = 1$ ) are slightly larger as compared with the observed full width, which

TABLE VI. Calculated decay widths of the  $\Lambda_c^*(2765) \rightarrow \Sigma_c(2455)\pi$  and  $\rightarrow \Sigma_c^*(2520)\pi$ . The quantum numbers of the  $\lambda$ - and  $\rho$ -modes are indicated by  $(n_\lambda, \ell_\lambda)$  and  $(n_\rho, \ell_\rho)$ , and  $J_{\Lambda_c^*}(j)^P$  stands for the assigned spin and parity for  $\Lambda_c^*$  with the light-component spin  $j$ .  $[\Sigma_c^{(*)} \pi]^+$  denotes the isospin summed width calculated by using the isospin average masses  $M_{\Sigma_c} = 2453.5$  (MeV),  $M_{\Sigma_c^*} = 2518.1$  (MeV), and  $m_\pi = 138.0$  (MeV). The ratio  $R$  indicates the  $\Sigma_c^*/\Sigma_c$  defined in the text.

$\Lambda_c^*(2765)^+$ Decay width [ $M_{\Lambda_c^*} = 2766.6$ (MeV)]						
Decay channel	full	$[\Sigma_c^{(*)} \pi]_{\text{total}}$	$[\Sigma_c \pi]^+$	$[\Sigma_c^* \pi]^+$	$R$	
Experimental value $\Gamma_{\text{exp}}$ (MeV)	50 [24]	...	...	...	...	
Momentum of final particle $q$ (MeV/c)			265	197		
	$(n_\lambda, \ell_\lambda), (n_\rho, \ell_\rho)$	$J_{\Lambda_c^*}(j)^P$				
	(0,1), (0,0)	$1/2(1)^-$	65.1–146.3	61.2–140.2	3.9–6.1	0.044–0.064
		$3/2(1)^-$	52.2–104.2	7.9–11.9	44.3–92.4	5.6–7.8
	(0,0), (0,1)	$1/2(0)^-$	0	0	0	...
This work		$1/2(1)^-$	325.8–676.3	323.7–673.3	2.1–3.0	0.0044–0.0064
$\Gamma$		$3/2(1)^-$	210.4–413.5	4.2–5.8	206.2–407.7	49–70
(MeV)		$3/2(2)^-$	9.4–13.1	7.6–10.5	1.9–2.7	0.25–0.26
		$5/2(2)^-$	6.3–8.8	3.4–4.7	2.9–4.2	0.87–0.90
	(1,0), (0,0)	$1/2(0)^+$	1.6–4.5	0.86–2.49	0.78–1.98	0.79–0.91
	(0,2), (0,0)	$3/2(2)^+$	4.7–10.9	4.4–10.1	0.33–0.72	0.071–0.076
		$5/2(2)^+$	1.9–4.4	0.13–0.32	1.77–4.04	12.8–13.8

does not seem inconsistent if we consider the uncertainty of  $g_A^q$ . However, by taking into account contributions of decays into nonresonant three-body  $\Lambda\pi\pi$ , these  $\lambda$ -mode states will receive a larger full width, with which the possibility for them to be identified with  $\Lambda_c^*(2765)$  might decrease.

Among the considered assignments in this article, the other assignments  $J_{\Lambda_c^*}(j)^P = 1/2(0)^-, 1/2(0)^+, 3/2(2)^-, 3/2(2)^+, 5/2(2)^-,$  and  $5/2(2)^+$  cannot be excluded because the total  $\Sigma_c^{(*)}\pi$  decay width is consistent with the experimental value. The ratio  $R$ , however, takes a different value reflecting the structure of the  $\Lambda_c^*$  baryon, which will help to determine the quantum numbers.

## 2. $\Lambda_c^*(2880) \rightarrow \Sigma_c^{(*)}\pi$ decay

The  $\Lambda_c(2880)$  charmed baryon is observed in the  $\Lambda_c\pi\pi$  channel [40,45] as well as in the  $pD^0$  channel [47]. The spin is determined as  $5/2$  from the angular distribution of the decay into  $\Sigma_c(2455)\pi$  [40]. In PDG [24], the parity is assigned to be positive from the analysis of the  $\Sigma_c^*/\Sigma_c$  branching ratio in comparison with the prediction of the chiral perturbation [30] with the heavy quark symmetry [3]. However, as discussed in [30] a subtlety arises when calculating the ratio.

In Table VII we summarize the quark configurations considered here for  $\Lambda_c^*(2880)$ . By comparing the observed full width  $\Gamma_{\text{exp}} = 5.8$  MeV and the calculated total one-pion decay width, we can exclude all of the  $p$ -wave configurations with the negative parity including  $5/2^-$ . As for  $5/2^-$  with  $\rho$ -mode excitation, both of the decays  $\Lambda_c^*(5/2^-) \rightarrow \Sigma_c(1/2^+)\pi$  and  $\Lambda_c^*(5/2^-) \rightarrow \Sigma_c^*(3/2^+)\pi$  [( $j^P = 2^-$ )  $\rightarrow$  ( $j^P = 1$ ) $^+0^-$  in terms of the light spin] go through by  $d$ -wave, and the  $\Sigma_c^*/\Sigma_c$  ratio  $R$  is larger than unity as

$$R(5/2(2)^-; \rho) = 1.6\text{--}1.8, \quad (80)$$

which does not agree with the experimental value  $R = 0.225 \pm 0.062 \pm 0.010$  [40]. This conclusion is consistent with the chiral perturbation calculation with heavy quark symmetry [3,30].

For the spin-parity  $5/2^+$  case, we can consider five configurations as shown in Table VII; one  $d$ -wave excitation in  $\lambda$ -motion [ $5/2(2)^+$  with  $\ell_\lambda = 2$ , denoted by  $\lambda\lambda$ ], the one in  $\rho$ -motion [ $5/2(2)^+$  with  $\ell_\rho = 2$ , denoted by  $\rho\rho$ ], and three double- $p$ -wave excitations in the  $\lambda$ - and  $\rho$ -motions [ $J_{\Lambda}(j)_\ell^P = 5/2(2)_1^+, 5/2(2)_2^+, 5/2(3)_2^+$  where  $\vec{\ell} = \vec{\ell}_\lambda + \vec{\ell}_\rho$  with  $(\ell_\lambda, \ell_\rho) = (1, 1)$ , denoted by  $\lambda\rho$ ]. Some of these configurations give a decay width consistent with the observed full width  $\Gamma_{\text{exp}} = 5.8$  (MeV). As for the  $\Sigma_c^*/\Sigma_c$

TABLE VII. Calculated decay width of the  $\Lambda_c^*(2880) \rightarrow \Sigma_c(2455)\pi$  and  $\rightarrow \Sigma_c^*(2520)\pi$ . The quantum numbers of the  $\lambda$ - and  $\rho$ -modes are indicated by  $(n_\lambda, \ell_\lambda)$ ,  $(n_\rho, \ell_\rho)$ , and  $J_{\Lambda_c^*}(j)^P$  stands for the assigned spin for  $\Lambda_c^*$  with the light-component spin  $j$  and the parity  $P$ . For the  $\{(0, 1), (0, 1)\}$  configurations, we also show the total angular momentum  $\vec{\ell} = \vec{\ell}_\lambda + \vec{\ell}_\rho$  as a subscript  $\ell$  in  $J_{\Lambda_c^*}(j)_\ell^P$ .  $[\Sigma_c^{(*)}\pi]^+$  denotes the isospin summed width calculated by using the isospin-averaged masses  $M_{\Sigma_c} = 2453.5$  (MeV),  $M_{\Sigma_c^*} = 2518.1$  (MeV), and  $m_\pi = 138.0$  (MeV). The ratio  $R$  indicates the  $\Sigma_c^*/\Sigma_c$  defined in the text.

$\Lambda_c^*(2880)^+$ Decay width [ $M_{\Lambda^*} = 2881.53$ (MeV)]						
Decay channel	full	$[\Sigma_c^{(*)}\pi]_{\text{total}}$	$[\Sigma_c\pi]^+$	$[\Sigma_c^*\pi]^+$	$R$	
Experimental value $\Gamma_{\text{exp}}$ (MeV)	$5.8 \pm 1.1$ [24]				0.225 [40]	
Momentum of final particle $q$ (MeV/c)			375	315		
	$(n_\lambda, \ell_\lambda), (n_\rho, \ell_\rho)$	$J_{\Lambda}(j)^P$				
	(0,1), (0,0)	$1/2(1)^-$	111.9–254.8	76.9–204.0	35.0–50.8	0.25–0.46
		$3/2(1)^-$	129.6–248.8	37.7–52.1	91.9–196.7	2.4–3.8
	(0,0), (0,1)	$1/2(0)^-$	0	0	0	...
This work		$1/2(1)^-$	502.5–1129.7	483.9–1104.7	18.6–24.9	0.038–0.023
$\Gamma$		$3/2(1)^-$	439.3–919.5	20.0–25.6	419.3–893.9	21–35
(MeV)		$3/2(2)^-$	52.8–68.5	36.0–46.0	16.7–22.4	0.46–0.49
		$5/2(2)^-$	42.0–55.3	16.0–20.5	26.0–34.9	1.6–1.7
	(1,0), (0,0)	$1/2(0)^+$	3.7–13.5	1.3–5.6	2.4–7.9	1.4–1.8
	(0,2), (0,0)	$3/2(2)^+$	16.3–39.5	13.9–34.2	2.4–5.3	0.16–0.17
		$5/2(2)^+$	11.2–26.1	1.2–2.8	9.9–23.3	8.1–8.4
	(0,0), (1,0)	$1/2(0)^+$	16.5–40.2	7.0–18.2	9.5–22.1	1.2–1.4
	(0,0), (0,2)	$3/2(2)^+$	44.8–85.4	39.5–76.0	5.3–9.4	0.12–0.13
		$5/2(2)^+$	27.8–52.2	1.4–2.6	26.4–49.5	18.7–18.9
	$(n_\lambda, \ell_\lambda), (n_\rho, \ell_\rho)$	$J_{\Lambda}(j)_\ell^P$				
	(0,1), (0,1)	$5/2(2)_2^+$	51.7–109.6	1.8–3.5	49.9–106.1	27.5–30.1
		$5/2(2)_1^+$	0.63–1.68	0	0.63–1.68	( $\infty$ )
		$5/2(3)_2^+$	2.9–5.8	2.1–4.0	0.85–1.73	0.41–0.43

TABLE VIII. Calculated decay width of the  $\Lambda_c^*(2940) \rightarrow \Sigma_c(2455)\pi$  and  $\rightarrow \Sigma_c^*(2520)\pi$ . The quantum numbers of the  $\lambda$ - and  $\rho$ -modes are indicated by  $(n_\lambda, \ell_\lambda)$ ,  $(n_\rho, \ell_\rho)$ , and  $J_{\Lambda_c^*}(j)^P$  stands for the assigned spin for  $\Lambda_c^*$  with the light-component spin  $j$  and the parity  $P$ . For the  $\{(0, 1), (0, 1)\}$  configurations, we also show the total angular momentum  $\vec{\ell} = \vec{\ell}_\lambda + \vec{\ell}_\rho$  as a subscript  $\ell$  in  $J_{\Lambda_c^*}(j)_\ell^P$ .  $[\Sigma_c^{(*)}\pi]^+$  denotes the isospin summed width calculated by using the isospin-averaged masses  $M_{\Sigma_c} = 2453.5$  (MeV),  $M_{\Sigma_c^*} = 2518.1$  (MeV), and  $m_\pi = 138.0$  (MeV). The ratio  $R$  indicates the  $\Sigma_c^*/\Sigma_c$  defined in the text.

$\Lambda_c^*(2940)^+$ Decay width [ $M_{\Lambda^*} = 2939.3$ (MeV)]						
Decay channel	full	$[\Sigma_c^{(*)}\pi]_{\text{total}}$	$[\Sigma_c\pi]^+$	$[\Sigma_c^*\pi]^+$	$R$	
Experimental value $\Gamma$ (MeV)	$17_{-6}^{+8}$ [24]		(seen)	...		
Momentum of final particle $q$ (MeV/c)			427	369		
	$(n_\lambda, \ell_\lambda), (n_\rho, \ell_\rho)$	$J_{\Lambda}(j)^P$				
	(0,1), (0,0)	$1/2(1)^-$	144.8–313.8	73.8–215.4	71.0–98.4	0.46–0.96
		$3/2(1)^-$	182.2–332.0	65.4–85.7	116.8–246.3	1.8–2.9
	(0,0), (0,1)	$1/2(0)^-$				
This work		$1/2(1)^-$	557.0–1299.3	519.3–1250.9	37.6–48.3	0.039–0.072
$\Gamma$		$3/2(1)^-$	536.5–1152.9	34.6–42.2	501.8–1110.7	15–26
(MeV)		$3/2(2)^-$	96.2–119.4	62.3–75.9	33.9–43.5	0.54–0.57
		$5/2(2)^-$	80.4–101.4	27.7–33.7	52.7–67.7	1.9–2.0
	(1,0), (0,0)	$1/2(0)^+$	3.7–17.4	1.1–6.4	2.7–11.0	1.7–2.5
	(0,2), (0,0)	$3/2(2)^+$	24.9–61.7	20.1–51.0	4.8–10.8	0.21–0.24
		$5/2(2)^+$	19.8–46.6	2.8–5.9	17.1–40.7	6.2–6.9
	$(n_\lambda, \ell_\lambda), (n_\rho, \ell_\rho)$	$J_{\Lambda}(j)_\ell^P$				
	(0,1), (0,1)	$7/2(3)_2^+$	5.8–11.1	2.6–4.8	3.2–6.2	1.22–1.29

ratio, however, we obtain considerably different values for different configurations like

$$\begin{aligned}
 R(5/2(2)^+; \lambda\lambda) &= 8.1\text{--}8.4, \\
 R(5/2(2)^+; \rho\rho) &= 18.7\text{--}18.9, \\
 R(5/2(2)_2^+; \lambda\rho) &= 27.5\text{--}30.1, \\
 R(5/2(2)_1^+; \lambda\rho) &= (\infty), \\
 R(5/2(3)_2^+; \lambda\rho) &= 0.41\text{--}0.43, \quad (81)
 \end{aligned}$$

where the ambiguities of model parameters are almost canceled. Note that  $(\infty)$  for the  $5/2(2)_1^+(\lambda\rho)$  state is due to the zero decay width into  $\Sigma_c\pi$ . Among these five configurations, we find that *only one* configuration [ $5/2(3)_2^+; \lambda\rho$ ] with the light spin  $j = 3$  with  $\ell = 2$  agrees both with the small ratio  $R < 1$  and with the magnitude of total decay width. This seems to contrast with the calculation in Ref. [30], where the other quark configuration for  $5/2^+$  also gives the small  $R$ .

This discrepancy can be explained as follows. The decay of  $\Lambda_c^*(5/2^+) \rightarrow \Sigma_c(1/2^+)\pi$  goes through only by the  $f$ -wave in the final two-body state, while the decay  $\Lambda_c^*(5/2^+) \rightarrow \Sigma_c^*(3/2^+)\pi$  can go through by both the  $f$ - and  $p$ -waves. The discussion based on the heavy quark limit leading to the model independent relation is possible only when the same  $f$ -waves are taken, which is completely contaminated by the presence of the  $p$ -wave contribution. As shown explicitly in Appendix B, the amplitude for  $\Lambda_c^*(5/2^+) \rightarrow \Sigma_c^*(3/2^+)\pi$  can contain the  $p$ -wave contribution [the  $c_1$  term in Eq. (B6)]. Thus we have

$$R(5/2^+) = \frac{\Gamma(\Sigma_c^*\pi)_p + \Gamma(\Sigma_c^*\pi)_d}{\Gamma(\Sigma_c\pi)_d} > 1, \quad (82)$$

except for the case of  $5/2(3)_2^+$ . For the case of  $5/2(3)_2^+$ , the  $p$ -wave contribution [the  $\tilde{c}_1$  term in Eq. (B7)] is zero because of the conservation of the spin-parity of the light component; the light system having  $j^P = 3^+$  cannot decay into that of  $1^+$  with the pion  $0^-$  in the  $p$ -wave, which leads to

$$R(5/2(3)_2^+; \lambda\rho) = \frac{\Gamma(\Sigma_c^*\pi)_d}{\Gamma(\Sigma_c\pi)_d} < 1. \quad (83)$$

We stress here again that the  $p$ -wave suppression is found only in the case of  $5/2(3)^+$  with  $\ell = 2$ , and not in the other states with  $5/2^+$ . Here it is worth mentioning that the  $\mathcal{O}(q^1)$  contribution, which allows us to distinguish the possible quark configurations for the same spin-parity, appears only in the  $A^{\nabla\sigma}$  term arising from the axial-vector coupling  $\gamma_\mu\gamma_5$  of the pion.

If  $\Lambda_c^*(2880)$  is assigned as a  $\lambda\rho$ -mode state, a question arises as to where the  $\lambda\lambda$ -mode states with  $\ell_\lambda = 2$  are. Excitation energies of the  $\lambda\lambda$ -mode states are expected to be lower than those of the  $\lambda\rho$ -mode states. Other information such as production rates as discussed in Ref. [48] is helpful to solve this problem, for which an experimental measurement is planned in J-PARC [49].

### 3. $\Lambda_c(2940) \rightarrow \Sigma_c^{(*)}\pi$ decay

As for  $\Lambda_c^*(2940)$ , a narrow peak is observed both in the  $pD^0$  channel [47] and in the  $\Sigma_c\pi$  channel [40]. The total

width is  $\Gamma_{\text{exp}} = 17^{+8}_{-6}$  (MeV) [24]. The spin-parity is not determined.

In Table VIII, we show the calculated one-pion decay widths together with the considered quark configurations for  $\Lambda_c^*(2940)$ . In the previous section, we pointed out the possibility that  $\Lambda_c^*(2880)$  is a  $5/2(3)_2^+$  excitation. If this is the case, a new question arises: which  $Y_c$  baryon is the partner of the HQS doublet possessing  $7/2(3)_2^+$ ? To discuss the possibility of  $\Lambda_c^*(2940)$  being the doublet partner of  $\Lambda_c^*(2880)$ , we also show the one-pion decay width with the  $7/2(3)_2^+$  assignment for  $\Lambda_c^*(2940)$  in the last line of Table VIII. We can see that this assignment can be consistent with the experimental full width in [24] in the sense that the calculated total one-pion emission decay width does not exceed the reported full width. For the same reason, the negative parity assignments can be excluded for  $\Lambda_c^*(2940)$ . Similarly to other  $\Lambda_c^*$  baryons, the partial decay widths and/or the  $\Sigma_c^*/\Sigma_c$  ratio will help us to determine the quantum numbers and the possible quark configuration as well.

#### IV. SUMMARY

We have systematically evaluated the decay widths of the charmed baryons  $\Lambda_c^*(2595)$ ,  $\Lambda_c^*(2625)$ ,  $\Lambda_c^*(2765)$ ,  $\Lambda_c^*(2880)$ , and  $\Lambda_c^*(2940)$  into  $\Sigma_c(2455)\pi$  and  $\Sigma_c^*(2520)\pi$ , as well as  $\Sigma_c(2455)$  and  $\Sigma_c^*(2520)$  into  $\Lambda_c\pi$  within the non-relativistic quark model. We have emphasized the usefulness of working in the baryon wave functions constructed to be consistent with heavy quark symmetry. This provides various selection rules associated with the pion emission between light component of the baryons. Our findings are as follows:

- (i) For the low-lying  $\Lambda_c^*(2595)$  and  $\Lambda_c^*(2625)$  baryons the quark model descriptions as the  $\lambda$ -mode excitations with a spin-0 diquark can explain the decay properties very well.
- (ii) The derivative coupling derived from the axial-vector interaction of  $\pi qq$  is essentially important to produce the experimental decay rate of  $\Lambda_c^*(2595)$ .
- (iii) Only one quark configuration,  $J_{\Lambda_c^*}(j)^P = 5/2(3)_2^+$  for  $\Lambda_c^*(2880)$ , among the five possible  $5/2^+$  configurations can lead to a result consistent with the experimental data, while all other four configurations of  $5/2^+$  cannot if the  $p$ -wave is properly considered. We note that the HQS does not necessarily lead to the small decay ratio of  $\Gamma(\Sigma_c^*\pi)/(\Sigma_c\pi)$  for  $5/2^+$ . This fact calls attention to the discussion based on the HQS [3,30], which requires decays in only one partial wave.
- (iv) Having the above conclusion, we have discussed the possibility of  $\Lambda_c^*(2940)$  being the HQS doublet partner of  $\Lambda_c^*(2880)$  possessing  $7/2(3)_2^+$ . Here we emphasize that our results concerning the possible HQS doublet,  $\Lambda_c^*(2880)$  and  $\Lambda_c^*(2940)$ , can be reached with a  $jj$  coupling scheme which respects the heavy quark symmetry.

- (v) The ratios of  $\Gamma(\Sigma_c^*\pi)/\Gamma(\Sigma_c\pi)$  are considerably different for different quark configurations even if the baryon spin-parity is the same. This fact is particularly useful for knowing the structure of charmed baryons.

In this study, we have discussed the various constraints for the one-pion emission decays due to the selection rules associated with the conservation of the spin  $j$  of the light component in the baryons. We have to keep in mind, however, that there is still a small breaking of heavy quark symmetry for a charm quark. Studies along these lines will be left for future works.

In our discussions in the quark model, we have considered only the excitations of valence quarks. We expect that they provide a good description for low-lying states. For higher excitations, however, there may be other modes such as pair creations of quark and antiquark, gluon excitations, and so on. The former can be taken into account in the quark model by couplings to mesons or by unquenched configurations [50], and in effective hadron models by hadronic molecule configurations [51,52]. The present systematic studies will help us to know where and how these configurations beyond the quark model ones show up, which should be studied in future J-PARC experiments.

#### ACKNOWLEDGMENTS

The authors are grateful to Kiyoshi Tanida, Tetsuya Yoshida, and Qiang Zhao for various discussions and for their useful comments. This work is supported by Grants-in-Aid for Scientific Research from JSPS [Grant No. JP26400275(C) for H. Nagahiro, Grant No. JP15K17641 for S. Y., Grant No. JP26400273(C) for A. H., Grant No. JP16H02188(A) for H. Noumi, and Grant No. JP25247036(A) for M. O., S. Y., and A. H.].

#### APPENDIX A: HARMONIC OSCILLATOR WAVE FUNCTIONS

The radial functions  $R_{n\ell}(\zeta)$  are given as

$$R_{00}(\zeta) = \frac{2a_\zeta^{3/2}}{\pi^{1/4}} e^{-a_\zeta^2 \zeta^2/2}, \quad (\text{A1})$$

$$R_{01}(\zeta) = \left(\frac{8}{3}\right)^{1/2} \frac{a_\zeta^{5/2}}{\pi^{1/4}} \zeta, e^{-a_\zeta^2 \zeta^2/2}, \quad (\text{A2})$$

$$R_{02}(\zeta) = \left(\frac{16}{15}\right)^{1/2} \frac{a_\zeta^{7/2}}{\pi^{1/4}} \zeta^2, e^{-a_\zeta^2 \zeta^2/2}, \quad (\text{A3})$$

$$R_{10}(\zeta) = \frac{\sqrt{6}a_\zeta^{7/2}}{\pi^{1/4}} \left(1 - \frac{2}{3} a_\zeta^2 \zeta^2\right) e^{-a_\zeta^2 \zeta^2/2}, \quad (\text{A4})$$

where

$$a_\zeta = \sqrt{m_\zeta \omega_\zeta}. \quad (\text{A5})$$

The  $\zeta$  is either  $\lambda$  or  $\rho$ . The reduced masses of  $m_\lambda$  and  $m_\rho$  are defined in Eq. (6).

## APPENDIX B: MATRIX ELEMENTS

In this appendix, we summarize the concrete forms of the helicity amplitudes  $A_h$ .

### 1. Ground state $\Sigma_c$ decays

The amplitudes for the decays of  $\Sigma_c^{(*)} \rightarrow \Lambda_c(1/2^+)\pi^-$  are given by

$$\begin{aligned} -iA_{1/2}^{\nabla\sigma} &= G \frac{\omega_\pi}{m} c \left( \frac{1}{2} q_\lambda + q_\rho \right) F(q), \\ iA_{1/2}^{q\sigma} &= -G \frac{q}{m} c \left( \frac{M}{2m+M} \omega_\pi - 2m \right) F(q), \end{aligned} \quad (\text{B1})$$

where the coefficient  $c$  is given as

$$c = \begin{cases} -1/\sqrt{3} & \text{for } \Sigma_c(1/2^+), \\ \sqrt{2/3} & \text{for } \Sigma_c^*(3/2^+). \end{cases} \quad (\text{B2})$$

TABLE IX. Coefficients for the negative parity  $\Lambda_c^*$  decays in Eq. (B5).

$(n_\lambda, \ell_\lambda)$	$(n_\rho, \ell_\rho)$	$\lambda$ -mode excitation ( $\zeta = \lambda$ )			$c_0$	$c_2$
		$J_{\Lambda_c}(j)^P$	$J_{\Sigma_c}^P$	$h$		
(0,1), (0,0)	(0,0)	1/2(1) <sup>-</sup>	1/2 <sup>+</sup>	1/2	$-\frac{1}{\sqrt{2}}$	$\frac{1}{3\sqrt{2}}$
			3/2 <sup>+</sup>	1/2	0	$-\frac{1}{3}$
		3/2(1) <sup>-</sup>	1/2 <sup>+</sup>	1/2	0	$-\frac{1}{3}$
			3/2 <sup>+</sup>	1/2	$-\frac{1}{\sqrt{2}}$	$\frac{\sqrt{2}}{3}$
				3/2	$-\frac{1}{\sqrt{2}}$	0
(0,0), (0,1)	(0,1)	$\rho$ -mode excitation ( $\zeta = \rho$ )				
		1/2(0) <sup>-</sup>	1/2 <sup>+</sup>	1/2	0	0
			3/2 <sup>+</sup>	1/2	0	0
		1/2(1) <sup>-</sup>	1/2 <sup>+</sup>	1/2	2	$-\frac{1}{3}$
			3/2 <sup>+</sup>	1/2	0	$-\frac{1}{3\sqrt{2}}$
		3/2(1) <sup>-</sup>	1/2 <sup>+</sup>	1/2	0	$-\frac{1}{3\sqrt{2}}$
			3/2 <sup>+</sup>	1/2	2	$-\frac{1}{6}$
				3/2	2	$-\frac{1}{2}$
		3/2(2) <sup>-</sup>	1/2 <sup>+</sup>	1/2	0	$\frac{1}{\sqrt{10}}$
			3/2 <sup>+</sup>	1/2	0	$\frac{1}{2\sqrt{5}}$
		3/2	0	$-\frac{1}{2\sqrt{5}}$		
5/2(2) <sup>-</sup>	1/2 <sup>+</sup>	1/2	0	$\frac{1}{\sqrt{15}}$		
	3/2 <sup>+</sup>	1/2	0	$\frac{1}{\sqrt{30}}$		
		3/2	0	$\frac{1}{\sqrt{5}}$		

TABLE X. Coefficients for the positive parity  $\Lambda_c^*(J^+)$  decays with an  $s$ -wave ( $n_\zeta = 1$ ) or a  $d$ -wave ( $\ell_\zeta = 2$ ) in Eq. (B6).

$(n_\lambda, \ell_\lambda)$	$(n_\rho, \ell_\rho)$	$\lambda$ -mode excitation ( $\zeta = \lambda$ )			$c_1$	$c_3$
		$J_{\Lambda_c^*}(j)^P$	$J_{\Sigma_c^*}^P$	$h$		
(1,0), (0,0)	(0,0)	1/2(0) <sup>+</sup>	1/2 <sup>+</sup>	1/2	$\frac{1}{3\sqrt{2}}$	$-\frac{1}{6\sqrt{2}}$
			3/2 <sup>+</sup>	1/2	$-\frac{1}{3}$	$\frac{1}{6}$
		(0,2), (0,0)	3/2(2) <sup>+</sup>	1/2 <sup>+</sup>	1/2	$\frac{1}{3}\sqrt{\frac{5}{2}}$
			3/2 <sup>+</sup>	1/2	$-\frac{1}{6\sqrt{5}}$	$\frac{1}{3\sqrt{5}}$
			3/2	$-\frac{1}{2\sqrt{5}}$	0	
		5/2(2) <sup>+</sup>	1/2 <sup>+</sup>	1/2	0	$\frac{1}{2\sqrt{15}}$
			3/2 <sup>+</sup>	1/2	$\sqrt{\frac{3}{10}}$	$-\frac{1}{\sqrt{30}}$
			3/2	$\frac{1}{\sqrt{5}}$	0	
		$\rho$ -mode excitation ( $\zeta = \rho$ )				
(0,0), (1,0)	(1,0)	1/2(0) <sup>+</sup>	1/2 <sup>+</sup>	1/2	$\frac{\sqrt{2}}{3}$	$-\frac{1}{6\sqrt{2}}$
			3/2 <sup>+</sup>	1/2	$-\frac{2}{3}$	$\frac{1}{6}$
(0,0), (0,2)	(0,2)	3/2(2) <sup>+</sup>	1/2 <sup>+</sup>	1/2	$\frac{\sqrt{10}}{3}$	$-\frac{1}{3\sqrt{10}}$
			3/2 <sup>+</sup>	1/2	$-\frac{1}{3\sqrt{5}}$	$\frac{1}{3\sqrt{5}}$
				3/2	$-\frac{1}{\sqrt{5}}$	0
		5/2(2) <sup>+</sup>	1/2 <sup>+</sup>	1/2	0	$\frac{1}{2\sqrt{15}}$
			3/2 <sup>+</sup>	1/2	$\sqrt{\frac{6}{5}}$	$-\frac{1}{\sqrt{30}}$
			3/2	$\frac{2}{\sqrt{5}}$	0	

The factor  $G$  denotes the coupling constant and the normalizations as

$$G = \frac{g_A^q}{2f_\pi} \sqrt{2M_{\Lambda_c}} \sqrt{2M_{\Sigma_c^*}}, \quad (\text{B3})$$

and the function  $F(q)$  denotes the Gaussian form factor as

$$F(q) = e^{-q_\lambda^2/4a_\lambda^2} e^{-q_\rho^2/4a_\rho^2}. \quad (\text{B4})$$

### 2. Negative parity $\Lambda_c^*(J^-)$ decays

The amplitudes for the decays of the negative parity excitations with a  $p$ -wave of  $\Lambda_c^*(J^-) \rightarrow \Sigma_c^{(*)}\pi$  are given by

$$\begin{aligned} -iA_h^{\nabla\sigma} &= iG \frac{\omega_\pi}{m} \left\{ c_0 a_\zeta + c_2 \left( \frac{1}{2} q_\lambda + q_\rho \right) \frac{q_\zeta}{a_\zeta} \right\} F(q), \\ -iA_h^{q\sigma} &= iG \frac{q}{m} \left( \frac{M}{2m+M} \omega_\pi - 2m \right) (-1) c_2 \frac{q_\zeta}{a_\zeta} F(q), \end{aligned} \quad (\text{B5})$$

where the coefficients  $c_0$  and  $c_2$  are summarized in Table IX. The subscript  $\zeta$  is either  $\lambda$  or  $\rho$ , depending on the  $\lambda$ - or  $\rho$ -mode excitations.

### 3. Positive parity $\Lambda_c^*(J^+)$ decays

The amplitudes for the decays of the positive parity excitations with an  $s$ -wave ( $n_\zeta = 1$ ) or a  $d$ -wave ( $\ell_\zeta = 2$ ) of  $\Lambda_c^*(J^+) \rightarrow \Sigma_c^{(*)} \pi$  are given by

$$\begin{aligned} -iA_h^{\nabla,\sigma} &= G \frac{\omega_\pi}{m} \left\{ c_1 q_\zeta + c_3 \left( \frac{1}{2} q_\lambda + q_\rho \right) \frac{q_\zeta^2}{a_\zeta^2} \right\} F(q), \\ -iA_h^{q,\sigma} &= G \frac{q}{m} \left( \frac{M}{2m+M} \omega_\pi - 2m \right) (-1) c_3 \frac{q_\zeta^2}{a_\zeta^2} F(q), \end{aligned} \quad (\text{B6})$$

where the coefficients  $c_1$  and  $c_3$  are summarized in Table X. The subscript  $\zeta$  is either  $\lambda$  or  $\rho$ , depending on the  $\lambda$ - or  $\rho$ -mode excitations.

The amplitudes for the decays of the positive parity excitations with  $\lambda - \rho$  mixed excited states  $(\ell_\lambda, \ell_\rho) = (1, 1)$  of  $\Lambda_c^*(J^+) \rightarrow \Sigma_c^{(*)} \pi$  are given by

$$\begin{aligned} -iA_h^{\nabla,\sigma} &= G \frac{\omega_\pi}{m} \left\{ \tilde{c}_1 \left( (-1)^\ell 2a_\rho \frac{q_\lambda}{a_\lambda} + a_\lambda \frac{q_\rho}{a_\rho} \right) + \tilde{c}_3 \frac{q_\lambda q_\rho}{a_\lambda a_\rho} \left( \frac{1}{2} q_\lambda + q_\rho \right) \right\} F(q), \\ -iA_h^{q,\sigma} &= G \frac{q}{m} \left( \frac{M}{2m+M} \omega_\pi - 2m \right) (-1) \tilde{c}_3 \frac{q_\lambda q_\rho}{a_\lambda a_\rho} F(q), \end{aligned} \quad (\text{B7})$$

where  $\ell$  denotes the total angular momentum  $\vec{\ell} = \vec{\ell}_\lambda + \vec{\ell}_\rho$  and the coefficients  $\tilde{c}_1$  and  $\tilde{c}_3$  are summarized in Table XI.

TABLE XI. Coefficients for the positive parity  $\Lambda_c^*(J^+)$  decays with  $\lambda - \rho$  mixed excitations in Eq. (B7).  $\ell$  denotes the total angular momentum defined by  $\vec{\ell} = \vec{\ell}_\lambda + \vec{\ell}_\rho$ .

$(n_\lambda, \ell_\lambda)$ $(n_\rho, \ell_\rho)$		$\lambda - \rho$ mixed excitation			$\tilde{c}_1$	$\tilde{c}_3$
$J_{\Lambda_c^*}(j)^P$	$\ell$	$J_{\Sigma_c^{(*)}}^P$	$h$			
(0,1), (0,1)	5/2(2) <sup>+</sup>	2	1/2 <sup>+</sup>	1/2	0	$\frac{1}{3} \sqrt{\frac{1}{5}}$
			3/2 <sup>+</sup>	1/2	$-\frac{3}{2} \sqrt{\frac{1}{10}}$	$\frac{1}{3} \sqrt{\frac{1}{10}}$
			3/2 <sup>+</sup>	3/2	$-\frac{3}{2} \sqrt{\frac{1}{15}}$	$\frac{1}{\sqrt{15}}$
		1	1/2 <sup>+</sup>	1/2	0	0
			3/2 <sup>+</sup>	1/2	$-\frac{1}{2} \sqrt{\frac{3}{10}}$	0
			3/2 <sup>+</sup>	3/2	$-\frac{1}{2} \sqrt{\frac{1}{5}}$	0
5/2(3) <sup>+</sup>	2	1/2 <sup>+</sup>	1/2	0	$-\frac{2}{3} \sqrt{\frac{2}{35}}$	
			3/2 <sup>+</sup>	1/2	0	$-\frac{2}{3} \sqrt{\frac{1}{35}}$
			3/2 <sup>+</sup>	3/2	0	$\sqrt{\frac{2}{105}}$
7/2(3) <sup>+</sup>	2	1/2 <sup>+</sup>	1/2	0	$-\sqrt{\frac{2}{105}}$	
			3/2 <sup>+</sup>	1/2	0	$-\frac{1}{\sqrt{105}}$
			3/2 <sup>+</sup>	3/2	0	$-\frac{1}{\sqrt{21}}$

### APPENDIX C: MATRIX ELEMENTS IN THE HEAVY QUARK LIMIT

In this appendix, we derive the matrix elements in the heavy quark limit to show how and when the geometric factor is separated, leading to the model independent relations [3]. Let us consider one-pion emission of a heavy baryon containing one heavy quark  $Q$  and a pair of light quarks  $qq$ . Following the notation in this paper, let the initial baryon denoted by  $\Lambda_Q$  and the final one by  $\Sigma_Q$ . Then the spin and angular momentum couplings for the initial  $\Lambda_c$  and final  $\Sigma_c \pi$  states are

$$\begin{aligned} |i\rangle &= |\Lambda_c\rangle = [j_{\Lambda_Q}, s_Q]^{J_{\Lambda_c} M_{\Lambda_Q}}, \\ |f\rangle &= |\Sigma_c \pi\rangle = [Y_L, [j_{\Sigma_Q}, s_Q]^{J_{\Sigma_Q}}]^{J_f M_f}, \end{aligned} \quad (\text{C1})$$

where  $J_{\Lambda_Q, \Sigma_Q}$  is the baryon spin,  $j_{\Lambda_Q, \Sigma_Q}$  the total spin of the light degrees of freedom,  $L$  the relative angular momentum of  $\pi \Sigma_Q$ , and  $J_f$  the total spin  $J_{\Sigma_Q} + L$ . The decay probability is then computed as

$$\Gamma \sim \sum_L |\langle f | \mathcal{L}_{\text{int}} | i \rangle|^2, \quad (\text{C2})$$

where  $\mathcal{L}_{\text{int}}$  is the pion-quark interaction, and the sum over the final state is taken over possible  $L$ 's. For instance, for the decay of  $5/2^+ \rightarrow 3/2^+$ , the angular momentum  $L$  can be both 1 ( $P$ -wave) and 3 ( $F$ -wave), while for the decay of  $5/2^+ \rightarrow 1/2^+$ , only the  $F$ -wave is possible.

In the literature, the model independent relation has been discussed for the ratio of the decays into  $\Sigma_c^*(3/2^+)$  and into  $\Sigma_c(1/2^+)$ . In the heavy quark limit it can be obtained only

for the decay into the same and single partial wave  $L$ . As we have discussed in Sec. IV D in detail, this is possible only in some limited cases where a selection rule due to the diquark transitions imposes an additional constraint. For a single  $L$ , after recoupling the final state, we obtain the matrix element as follows:

$$\begin{aligned} & \langle [Y_L, [j_{\Sigma_Q}, s_Q]^{J_f M_f}]^{J_f M_f} | \mathcal{L}_{\text{int}} | [j_{\Lambda_Q}, s_Q]^{J_{\Lambda_Q} M_{\Lambda_Q}} \rangle \\ &= \sum_{j_f} \hat{J}_{\Sigma_Q} \hat{j}_f (-1)^{j_{\Sigma_Q} + s_Q + J_f + L} \begin{Bmatrix} J_{\Sigma_Q} & j_{\Sigma_Q} & s_Q \\ j_f & J_f & L \end{Bmatrix} \\ & \times \langle [[Y_L, j_{\Sigma_Q}]^{j_f}, s_Q]^{J_f M_f} | \mathcal{L}_{\text{int}} | [j_{\Lambda_Q}, s_Q]^{J_{\Lambda_Q} M_{\Lambda_Q}} \rangle. \quad (\text{C3}) \end{aligned}$$

Because the interaction  $\mathcal{L}_{\text{int}}$  is active only for the light quarks, after the application of the Wigner-Eckart theorem, the matrix element in the third line can be factorized into one of the light degrees of freedom,  $\langle [Y_L, j_{\Sigma_Q}]^{j_f} | \mathcal{L}_{\text{int}} | j_{\Lambda_Q} \rangle$ , and the trivial one of the heavy quark. If, furthermore, the configuration of the light degrees of freedom is uniquely determined, which is to fix  $j_f$  at a single value, the  $J_{\Sigma_Q}$  dependence is completely dictated by the six- $j$  symbol and the normalization  $\hat{J}_{\Sigma_Q}$ . This explains how and when the ratio in Eq. (75) can be determined in a model independent manner by the formula (C3).

- 
- [1] S. Weinberg, *Phys. Rev.* **130**, 776 (1963); **137**, B672 (1965).  
[2] H. Nagahiro and A. Hosaka, *Phys. Rev. C* **90**, 065201 (2014).  
[3] N. Isgur and M. B. Wise, *Phys. Rev. Lett.* **66**, 1130 (1991).  
[4] M. Neubert, *Phys. Rep.* **245**, 259 (1994).  
[5] S. Yasui and K. Sudoh, *Phys. Rev. D* **80**, 034008 (2009).  
[6] Y. Yamaguchi, S. Ohkoda, S. Yasui, and A. Hosaka, *Phys. Rev. D* **85**, 054003 (2012).  
[7] Y. Yamaguchi, S. Ohkoda, S. Yasui, and A. Hosaka, *Phys. Rev. D* **84**, 014032 (2011).  
[8] Y. Yamaguchi, S. Yasui, and A. Hosaka, *Nucl. Phys.* **A927**, 110 (2014).  
[9] C. Garcia-Recio, V.K. Magas, T. Mizutani, J. Nieves, A. Ramos, L. L. Salcedo, and L. Tolos, *Phys. Rev. D* **79**, 054004 (2009).  
[10] D. Gamermann, C. Garcia-Recio, J. Nieves, L. L. Salcedo, and L. Tolos, *Phys. Rev. D* **81**, 094016 (2010).  
[11] C. Garcia-Recio, J. Nieves, O. Romanets, L. L. Salcedo, and L. Tolos, *Phys. Rev. D* **87**, 034032 (2013).  
[12] Y. Yamaguchi, S. Ohkoda, A. Hosaka, T. Hyodo, and S. Yasui, *Phys. Rev. D* **91**, 034034 (2015).  
[13] Y.-R. Liu and M. Oka, *Phys. Rev. D* **85**, 014015 (2012).  
[14] S. Maeda, M. Oka, A. Yokota, E. Hiyama, and Y.-R. Liu, *Prog. Theor. Exp. Phys.* **2016**, 023D02 (2016).  
[15] S. Yasui, K. Sudoh, Y. Yamaguchi, S. Ohkoda, A. Hosaka, and T. Hyodo, *Phys. Lett. B* **727**, 185 (2013).  
[16] S. Yasui and K. Sudoh, *Phys. Rev. C* **87**, 015202 (2013).  
[17] S. Yasui and K. Sudoh, *Phys. Rev. C* **89**, 015201 (2014).  
[18] S. Yasui, *Phys. Rev. D* **91**, 014031 (2015).  
[19] D. Suenaga, B.-R. He, Y.-L. Ma, and M. Harada, *Phys. Rev. C* **89**, 068201 (2014).  
[20] D. Suenaga, B.-R. He, Y.-L. Ma, and M. Harada, *Phys. Rev. D* **91**, 036001 (2015).  
[21] D. Suenaga and M. Harada, *Phys. Rev. D* **93**, 076005 (2016).  
[22] A. Hosaka, T. Hyodo, K. Sudoh, Y. Yamaguchi, and S. Yasui, [arXiv:1606.08685](https://arxiv.org/abs/1606.08685)  
[23] T. Yoshida, E. Hiyama, A. Hosaka, M. Oka, and K. Sadato, *Phys. Rev. D* **92**, 114029 (2015).  
[24] K. A. Olive *et al.* (Particle Data Group Collaboration), *Chin. Phys. C* **38**, 090001 (2014).  
[25] T.-M. Yan, H.-Y. Cheng, C.-Y. Cheung, G.-L. Lin, Y. C. Lin, and H.-L. Yu, *Phys. Rev. D* **46**, 1148 (1992); **55**, 5851(E) (1997).  
[26] P. L. Cho, *Phys. Lett. B* **285**, 145 (1992).  
[27] P. L. Cho, *Phys. Rev. D* **50**, 3295 (1994).  
[28] J. L. Rosner, *Phys. Rev. D* **52**, 6461 (1995).  
[29] C. Albertus, E. Hernandez, J. Nieves, and J. M. Verde-Velasco, *Phys. Rev. D* **72**, 094022 (2005).  
[30] H.-Y. Cheng and C.-K. Chua, *Phys. Rev. D* **75**, 014006 (2007).  
[31] X.-H. Zhong and Q. Zhao, *Phys. Rev. D* **77**, 074008 (2008).  
[32] F. Hussain, J. G. Korner, and S. Tawfiq, *Phys. Rev. D* **61**, 114003 (2000).  
[33] J. G. Korner, M. Kramer, and D. Pirjol, *Prog. Part. Nucl. Phys.* **33**, 787 (1994).  
[34] L. A. Copley, N. Isgur, and G. Karl, *Phys. Rev. D* **20**, 768 (1979).  
[35] D. Pirjol and T.-M. Yan, *Phys. Rev. D* **56**, 5483 (1997).  
[36] H. Albrecht *et al.* (ARGUS Collaboration), *Phys. Lett. B* **317**, 227 (1993).  
[37] K. W. Edwards *et al.* (CLEO Collaboration), *Phys. Rev. Lett.* **74**, 3331 (1995).  
[38] T. Aaltonen *et al.* (CDF Collaboration), *Phys. Rev. D* **84**, 012003 (2011).  
[39] P. L. Frabetti *et al.* (E687 Collaboration), *Phys. Rev. Lett.* **72**, 961 (1994).  
[40] K. Abe *et al.* (Belle Collaboration), *Phys. Rev. Lett.* **98**, 262001 (2007).  
[41] S. Weinberg, *Phys. Rev. Lett.* **65**, 1181 (1990).  
[42] S. Weinberg, *Phys. Rev. Lett.* **67**, 3473 (1991).  
[43] M. A. Morrison and G. A. Parker, *Aust. J. Phys.* **40**, 465 (1987).  
[44] A. Chodos, R. L. Jaffe, K. Johnson, and C. B. Thorn, *Phys. Rev. D* **10**, 2599 (1974).  
[45] M. Artuso *et al.* (CLEO Collaboration), *Phys. Rev. Lett.* **86**, 4479 (2001).  
[46] H. Nagahiro and A. Hosaka (to be published).

- [47] B. Aubert *et al.* (BABAR Collaboration), *Phys. Rev. Lett.* **98**, 012001 (2007).
- [48] S.-H. Kim, A. Hosaka, H.-C. Kim, H. Noumi, and K. Shirotori, *Prog. Theor. Exp. Phys.* **2014**, 103D01 (2014).
- [49] H. Noumi *et al.*, J-PARC Proposal P50, 2012.
- [50] R. Bijker, J. Ferretti, and E. Santopinto, *Phys. Rev. C* **85**, 035204 (2012).
- [51] T. Mizutani and A. Ramos, *Phys. Rev. C* **74**, 065201 (2006).
- [52] J. Haidenbauer, G. Krein, U.-G. Meissner, and L. Tolos, *Eur. Phys. J. A* **47**, 18 (2011).